

Measurement of Underwater Sound at the GEMINI Windpark Site

Dr. Klaus Lucke

Centre for Marine Science and Technology, Curtin University, Perth, Australia

Contents

Disclaimer.....	3
Summary.....	5
Introduction	7
Analysing Underwater Sound	8
Ambient noise.....	10
Methods	11
Instrumentation.....	11
Recording Sites and Sampling Regime	12
Data Processing	13
Data Review	13
Results	15
Sound sources	20
Quantitative analysis of noise levels	40
Discussion	47
Conclusion	47
References.....	49
Appendix A	51

Unpublished research report delivered to Gemini Windpark, Amstelveenseweg 760, 1081 JK Amsterdam
THE NETHERLANDS.

To be cited as: Lucke, Klaus (2015) Measurement of underwater sound at the GEMINI Windpark site.
Unpublished Report, Centre for Marine Science and Technology, Curtin University, Perth, Australia. Pp53.

Disclaimer

The monitoring of underwater sound in the vicinity of Gemini offshore windpark, in the period prior to construction, formed part of a larger project to record base-line data on the surrounding habitat, specifically in relation to cetaceans. The most common cetacean in the area is the harbour porpoise (*Phocoena phocoena*). The contract for the overall project was undertaken by the Institute for Marine Resources and Ecosystem Studies (IMARES – Wageningen University Research), The Netherlands.

Dr Klaus Lucke was an employee of IMARES when the contract commenced, and project leader of the underwater sound and passive acoustics monitoring programs until he commenced employment with Curtin University in November 2014. All the planning, field work and management of the project was performed by IMARES staff, including Dr Lucke.

On Dr Lucke's departure from IMARES, management for the project was taken over by other IMARES staff, and IMARES staff completed the deployment and retrieval programs for the underwater sound loggers. As an employee of Curtin University, Dr Lucke was sub-contracted by IMARES to analyse and interpret the data from the underwater sound loggers, and draft the report. IMARES assisted in reviewing the report and, as part of their contract, supplied the report to Gemini.



Jakob Asjes,

IMARES Ecosystems Department

January 2016

Summary

This report provides a summary of underwater noise measurements conducted in 2013 and 2014. The key findings based on the preliminary analysis of the collected data are as follows:

1. Sea noise measurements made at the two sites, GEMINI 1, 40 km west from the Gemini windpark, and GEMINI 8, between the two halves of the Gemini windpark, provide information on ambient noise in the area. Anthropogenic sources of underwater noise, in particular, shipping traffic, a geotechnical survey, and pile driving sound, were the major contributors to the noise environment in the area.
2. The underwater noise environment at GEMINI 1 (more easterly of the two positions) is more heavily dominated by shipping noise, mechanical noise – presumably associated with trawling. Shipping noise was highly variable in intensity and comprised noises from both near and distant vessels. Even though pile driving noise from construction of windparks in adjacent German waters was recorded at higher levels at station GEMINI 8, periods of intense noise from pile driving were evident in recordings from both positions. Additional information is required on piling locations and times from the operators for a more comprehensive analysis and more definite conclusion on the contribution made by these operations to ambient noise.
3. Sounds of biological origin were rarely evident in the datasets. This can partly be attributed to the frequency range of these recordings, which was limited to 24 kHz to compensate for energy and data storage demands thus eliminating sounds produced by harbour porpoises. Fish sounds, such as choruses produced by fish in tropical regions, were not expected and have not been detected in any of the recordings.
4. Noise recorded at both stations was up to 20 dB higher in certain frequency bands during periods when there was man-made noise than during periods when man-made noise was absent. On average, over the entire period, there was approximately a 5-10 dB difference between the two noise logger stations over most of the frequency band. In 2013, noise levels from GEMINI 1 were, on average, higher than those from GEMINI 8 while the recordings from 2014 provide a reverse result.
5. Several underwater explosions were detected in the recordings from both stations. These acoustic events have the potential to adversely affect marine animals.
6. This report provides a description of back-ground noise (a base-line), both anthropogenic and natural, against which noise produced during construction and operation of the windpark can be compared. The report is largely descriptive of the types of noise present prior to construction of Gemini windpark. More detailed analysis and interpretation of potential impacts can be conducted on obtaining noise profiles during construction and operation.

Introduction

The planned construction and operation of wind turbines at the GEMINI windpark in Dutch waters includes several activities which have the potential or have proven to cause underwater sound emissions. The Dutch company IMARES (Institute for Marine Ecosystems Research) has been contracted by Gemini windpark to undertake pre-construction monitoring of the environment in the vicinity of the windpark. As part of that monitoring, IMARES deployed and retrieved underwater noise loggers to obtain records of background sounds, including of anthropogenic origin. IMARES have subcontracted the Centre for Marine Science and Technology, Curtin University (Perth, Australia), to undertake analysis of the noise logger data. This facilitated project management by Klaus Lucke, who was employed by IMARES during the planning and deployment of the noise loggers and, since 2014, has been employed by Curtin University.

An important consideration of anthropogenic underwater noise production is that it has a high potential to impact on marine mammals. Many facets of windpark construction produce underwater noise, but the activity with the greatest potential to impact on marine mammals is likely to be pile-driving of the turbine towers into the sediment. In the Gemini windpark area, the most commonly occurring marine mammals are harbour porpoises (*Phocoena phocoena*) as well as harbour seals (*Phoca vitulina*) and grey seals (*Halichoerus grypus*).

Marine mammals perceive their marine environment mainly via their acoustic sense. Underwater sound is for these animals the most important trigger for behavioural reactions. In order to link any detected effect of the construction and operation of the wind turbines on the presence and distribution of the marine mammals, it is essential to record and analyse the overall underwater sound regime (i.e. the soundscape) in the area. These recordings are the only means to comprehensively assess the cause-effect relationship and especially to exclude other, non wind farm related activities (shipping, fishing, other constructions, sonars etc.) as potential external causes for any documented changes in the behaviour or presence and distribution of the animals.

Here I present the results by means of two autonomous underwater noise recorders deployed at two CPOD stations in the offshore area north of the Dutch coast, one within or between the wind farms, the other at approximately 40 km west of the planned GEMINI windpark.

The aim of the noise logger study is to achieve continuous acoustic recordings of the underwater noise within the windpark area as well as at a reference position outside of this area before the construction of the wind turbines commences. The underlying hypothesis is that especially the construction related activities will generate strong and clearly identifiable acoustic emissions into the marine environment which can be recorded and analysed by means of acoustic noise loggers. The operation of the wind turbines may possibly as well contribute to the overall soundscape, but would hardly be recognisable, identifiable and quantifiable as a single sound type. In order to determine the change in the soundscape due to the additional contribution by either type of the GEMINI windpark related activity, it is essential to have this baseline data.

The data presented here will describe the underwater soundscape in a situation prior to the construction of the wind turbines. These sounds can be of natural origin such as wave agitation and currents, but in addition there are also numerous anthropogenic sound sources creating and emitting sound into the North Sea. Hence, the baseline situation prior to construction is not an undisturbed situation. Moreover, as with the construction activities, most natural and anthropogenic sound sources emit sound intermittently and in an irregular pattern which will make it difficult to identify and quantify each acoustic contribution, both during the baseline as well as any future sound monitoring. Nevertheless, the underwater sound recordings will allow detection and possibly identification of sound sources which would remain undetected otherwise.

Analysing Underwater Sound

Underwater noise analysis is a specialist field and to improve interpretation of the results for the general reader, a brief description of the measurement of underwater noise is provided below.

Sound is mediated in air and in water by means of pressure changes, i.e. a compression is followed by a rarefaction. The hearing system of humans as well as marine mammals is capable of converting this mechanical event into the perception of a sound.

While a normal tone has a specific pitch, i.e. a clear tone-height, a normal sound covers a wide frequency range at any point in time. This frequency range as well as the pitch of this sound can change over time, thereby changing the sound as we would perceive it.

Sound can be described and visualised in terms of its pressure or the energy contained in the signal. The difference is (basically) that the pressure is denoted as sound pressure level (SPL) in 'dB re μPa '. The SPL describes the maximum positive and negative peak of the pressure wave (occurring at a very specific moment in time). The so-called waveform display is the graphical representation of this sound pressure which changes quickly over time (see Figure 1).

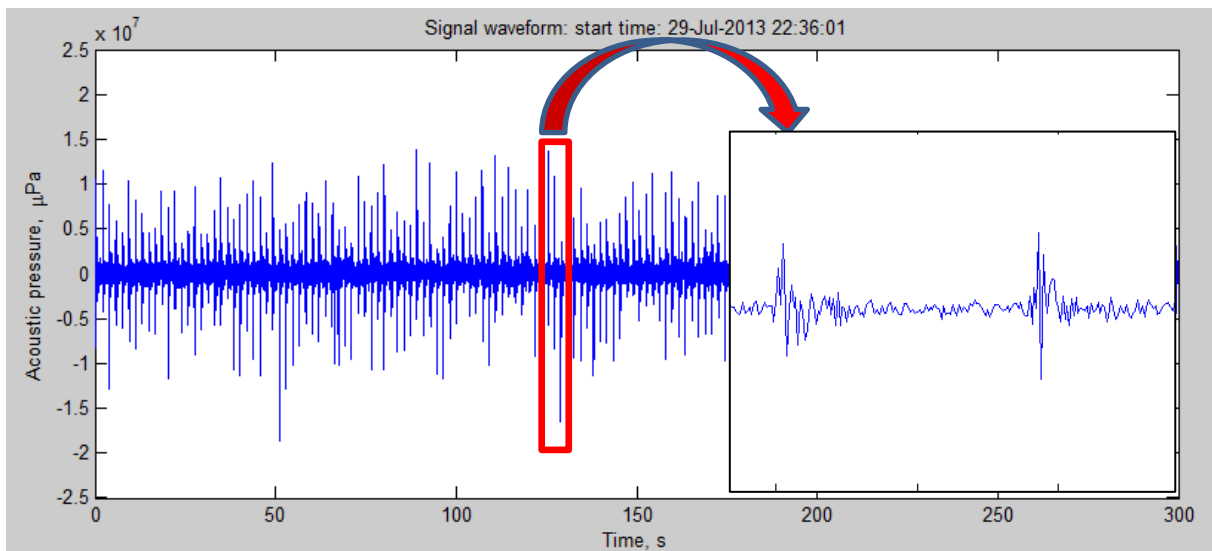


Figure 1: Waveform of a series of pile driving impulses (larger figure) and zoomed in the waveform of two individual pile driving impulses (smaller figure). Time in seconds is displayed on the x-axis and the pressure (or amplitude) of the sound on the y-axis of both figures.

The energy contained in sound can be visualised in a spectrogram as exemplified in Figure 2.

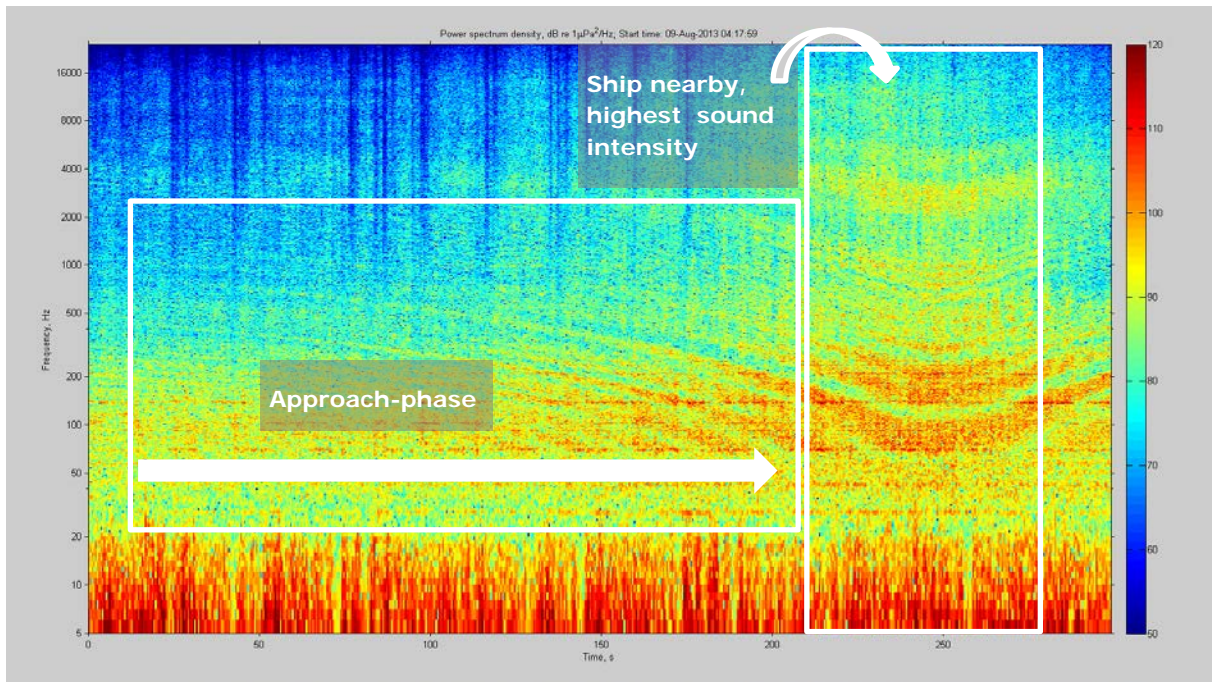


Figure 2: Spectrogram of a ship passage along the recording hydrophone/ noise logger. Time is displayed on the x-axis, the frequency on a logarithmic scale (kHz) on the y-axis. The power spectrum density (colour-coded, see legend on the right) is integrated over 1 s and displayed in dB re $1 \mu\text{Pa}^2/\text{Hz}$.

With decreasing distance to the recording noise logger the energy of the ship's sound is increasing, represented by colours changing from blue over green, yellow and orange to red (highest intensity). The curved pattern of the lines is known as a Lloyd's mirror interference pattern, where the vessel's closest point of approach is at the local minimum. The ship emits very broadband (Gaussian and white) noise. As a function of range, some frequencies cancel out destructively others add constructively (i.e. Lloyd's mirror effect). It just appears in the spectrogram as if frequencies are downsweeping before and upsweeping after the passage of the ship, but that's not really the case. The Lloyd's mirror effect is based on the constructive and destructive interference of the direct path arrival of the signal and the destructive (out-of-phase) arrival of the signal after being reflected at the surface (Carey 2009), causing a spectral pattern as can be seen in figure 2.

The sound energy is denoted as sound exposure level (SEL) and the unit is dB re $1 \mu\text{Pa}^2\text{s}$. There are many more details to consider, especially with regard to the correct terminology, but within the scope of this report it is sufficient to keep the terminology constant without going into more detail.

Throughout the report the different sounds are presented by one or several of these types of displays to emphasize either the temporal structure (changing amplitude over time) or the change of the sound energy distribution over time.

All data presented in this report are acoustically unweighted and can be reported in other metrics (such as: sound pressure level (SPL) for continuous sound, sound exposure level (SEL) for transient sounds and/or zero to peak sound pressure level (Lz-p) for transient sounds) if required (see De Jong et al. 2011, TSG Noise 2013). All those metrics can be extracted from the data as all sound recordings are calibrated through a number of calibration steps, including the calibration tone applied just before the instrument enters the water, and this provides an absolute output in frequency and intensity from which any metrics can be generated.

Ambient noise

The background noise in each marine area is a composite of noise from many sources near and far and differs regionally and seasonally. For deep water areas, Wenz (1962) collated the most relevant natural and anthropogenic contributors (Figure 3). While the received levels may differ in shallow water areas such as the study area, these curves are a good approximation for the relative contribution of each source to the ambient noise.

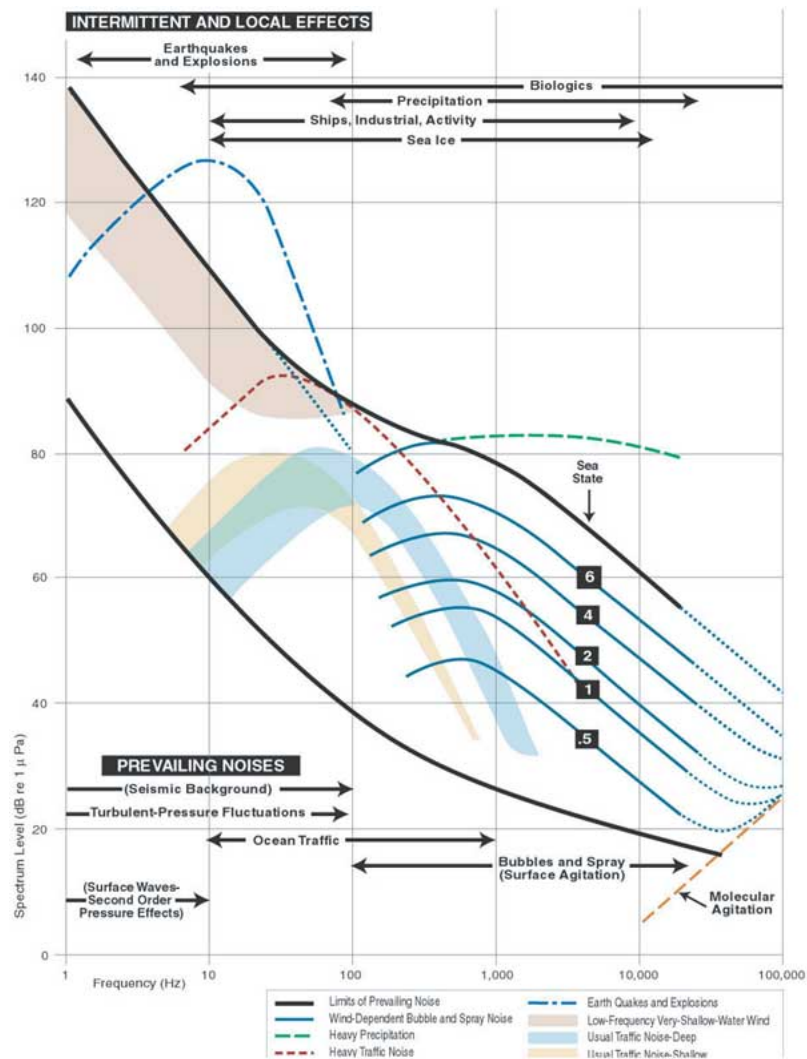


Figure 3: 'Wenz' curves describing pressure spectral density levels of marine ambient noise from weather, wind, geologic activity, and commercial shipping for deep water conditions (Ocean Studies Board 2003 adapted from Wenz 1962). Spectrum levels are plotted as a function of frequency. Black arrows indicate the frequency range covered by the sounds emitted from various sources. Thick black lines indicate limits of prevailing ambient noise. Sea state is a unit describing different wave heights (e.g. wind at Beaufort 4 = approx. sea state 3).

Methods

Instrumentation

The noise logger chosen for this study was the 'Autonomous Multi-Channel Recorder (AMAR G3, JASCO Research Ltd., Canada). The AMAR G3 is fitted with a single GTI-M8E hydrophone which has a nominal sensitivity of -164 dB re 1 V/ μ Pa and was set for a gain of 0 dB. The spectral density noise floor of the AMAR in this configuration is approximately 34 dB re 1 μ Pa/Hz. Its recording performance is dictated by the available data storage (1790 GB) on the one side and the battery power on the other side. The recorded frequencies range from 8 Hz to a maximum of 24 kHz. However, the amount of data increases in a linear way with the maximum frequency recorded (at a factor of 2).

We used continuous recording at the frequency range of 8 Hz to 24 kHz with a second battery pack, ensuring that no emission from a typical anthropogenic noise source was missed and that power did not run out within an envisaged service-interval of 100 - 120 days. An increased frequency range (maximum of 32 kHz) essentially would not provide more or new information on the presence of noise sources. Data were sampled at 24 bit resolution, stored as in digital format on the on-board AMAR solid state memory and it is not compressed (i.e. lossless).

Retrieving the data (almost 2 TB) from the logger takes >1 day and requires bringing the devices onto land. Each device was calibrated prior to and after each deployment using a pistonphone G.R.A.S. type $42AA$ equipped with a M8E coupler. The AMARs were chosen as they provide a reliability of almost 100% over the past years. Their resilience to intense acoustic impulses as during pile driving is sufficient for the positions chosen.



Figure 4. The noise logger (JASCO Applied Sciences).

Recording Sites and Sampling Regime

Two locations were chosen for the deployment of the noise loggers, one at the CPOD station GEMINI 8 in the centre between the two halves of the GEMINI wind farm to get a good signal-to-noise ratio (i.e. a good detectability, the 'near site'), and the other at the CPOD station GEMINI 1 at a distance of 40 km to the west of GEMINI 8 (the 'far site') (Figure 5). The coordinates of the two locations are:

BARD 1/ GEMINI 1: N 53° 58.84740; E 5° 14.83008

BARD 8/ GEMINI 8: N 54° 2.25660; E 5° 58.07202

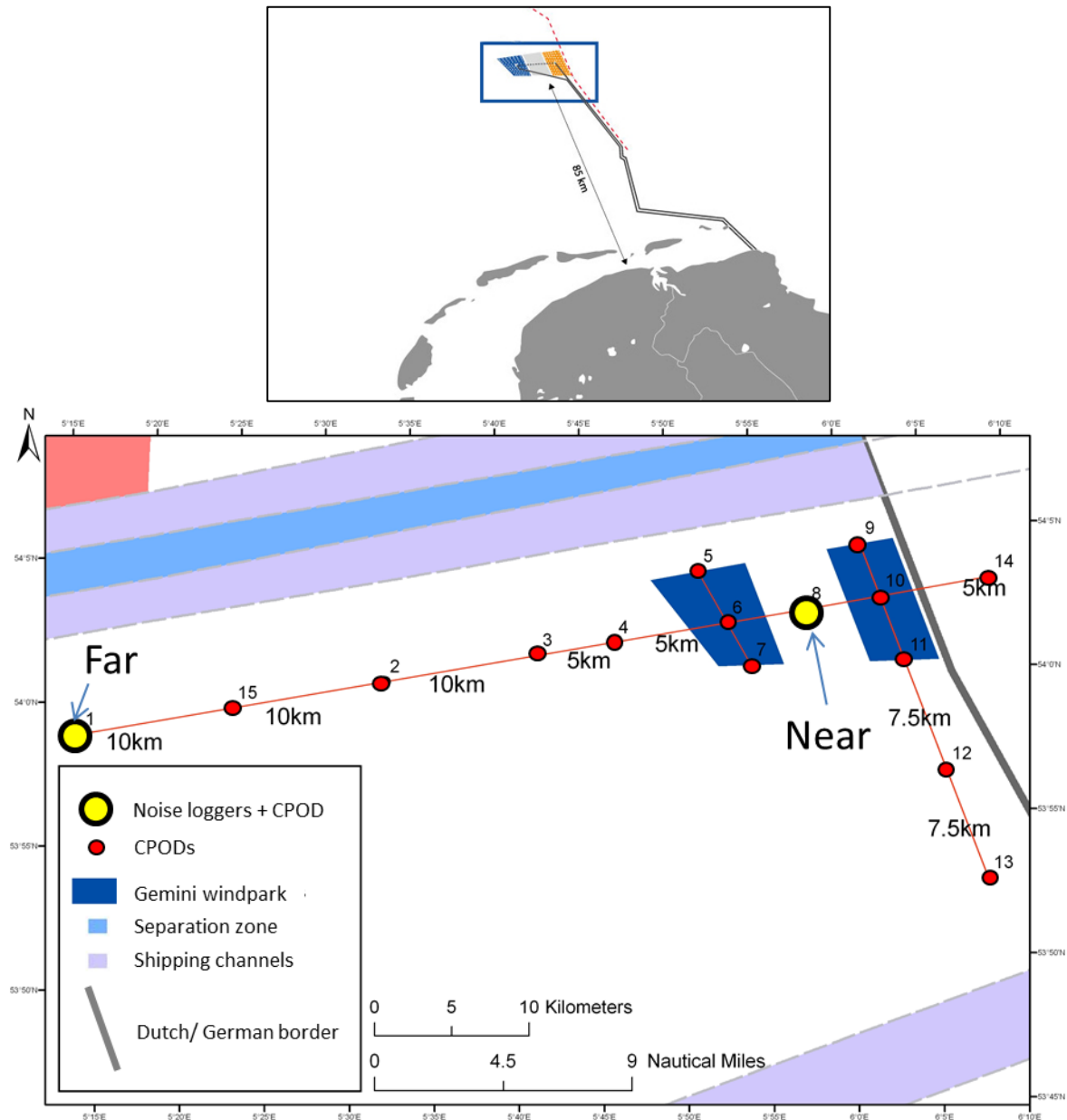


Figure 5: Location of the Gemini windpark area (upper graph) and the location of the AMAR noise logger sites in relation to CPOD deployment sites in the Gemini windpark area (lower graph).

The devices were bottom mounted and equipped with float collars ensuring a position of up to 5 m above the sea floor. The frequency range of the recordings is 10 Hz – 24 kHz, thus covering most of the human activities at sea (except most sonar activities). In 2013 and 2014 recordings were made continuously over the entire deployment period.

Table 1. Deployment locations and periods of the acoustic recorders and recording settings of the acquisition program.

Buoy #	AMAR #	Start of recording (dd/mm/yyyy)	End of recording (dd/mm/yyyy)	Duty cycle	Bandwidth [kHz]
Gemini 1	128	18/07/2013	29/09/2013	Continuous	24
Gemini 8	142	18/07/2013	29/09/2013	Continuous	24
Gemini 1	195		n.a.*	Continuous	24
Gemini 8	193		n.a.*	Continuous	24
Gemini 1	277	12/03/2014	03/07/2014	Continuous	24
Gemini 8	276	12/03/2014	15/06/2014	Continuous	24

*device lost, no data retrieved.

In this report the most relevant sound signatures of anthropogenic activities have been identified, analysed and described for the study period of July-September 2013 and March-July 2014. Two data sets from a deployment in winter 2013/14 could not be added as the devices were lost, most likely due to close passes of fishing (trawl) equipment stripping the AMARs from their moorings.

Data Processing

Processing and analysis of sea noise data involved two stages. Firstly, the power spectral density (PSD) of sea noise (or noise spectrum) was calculated for each recording. The PSD was corrected for the frequency response of the acoustic receiving system derived from the calibration data and for the hydrophone sensitivity so that the noise spectra and spectral levels were represented in absolute values. These spectra were used to plot long-term average spectrograms of sea noise. Such spectrograms were then used to visually review the main features of sea noise and their long-term variations in the second stage of data analysis. Secondly, a *Matlab* toolbox with a Graphic User Interface was developed to: 1) visualise sea noise spectrograms of low temporal resolution (long-term average spectrograms) for a chosen time period of several days; 2) select particular recording times based on the spectrogram features of interest, and; 3) analyse the waveform and spectrogram of sea noise within the individual recording made at the selected time. In this stage, the time-frequency characteristics of sea noise can be investigated in more detail using spectrograms of high resolution.

Acoustic units used for sea noise analysis and referred to in this report are described in the Glossary in Appendix A.

Data Review

For the purposes of this summary report, sea noise spectrograms obtained from the signal PSDs averaged over each individual recording of 30 minutes, were created with each panel representing time periods of multiple days, to visually examine the noise data for long-term variations. The spectrograms are displayed with a logarithmic frequency scale from 5 Hz to 24 kHz and a fixed colour scale bounded within 50 dB and 120 dB re 1 $\mu\text{Pa}^2/\text{Hz}$. The colour scale bounds were fixed so as to standardise the plots and optimise the colour dynamic range for the intensity of weak and strong signals observed in the dataset. These spectrograms demonstrate broad scale temporal patterns only and, because of the averaging involved, do not display individual signals which are short compared to the averaging time of 30 minutes. The spectrograms tend to highlight signal types which are either intense and/or persist across the averaging time (e.g. intense ship noise). Analyses depicting short-term acoustic events (e.g. explosions) were also done using *Adobe Audition* and are shown in enlarged sections at higher temporal resolution.

Results

Overall, noise of anthropogenic origin dominated the underwater noise environment in the monitored area. The major sources of this noise were various ships and boats moving past the two recording sites. In addition, there were shorter or longer periods of tonal or quasi-tonal noises containing several harmonics in some instances, which were most likely machinery noise from trawling vessels operating nearby (e.g. from on-board motors and pumps).

Periods of very intense tonal noise at low-to-mid frequencies lasting for several days occurred regularly from 22 August 2013 to 3 September 2013 (Figure 6). The origin of this was likely to be drilling activity for a geotechnical investigation at the projected construction site (personal communication, Luuk Folkerts, 25 Nov 2014).

Natural (physical) noises, such as noise from tidal current, wind and rain typical of the southern North Sea, were regularly clearly identifiable, but were sometimes masked by anthropogenic sounds.

Statistics of the spectrum level of noise recorded is demonstrated in Figure 6 and 7. The major variations in the noise spectrum level exceeding 20 dB were observed at frequencies from approximately 10 Hz to 1 kHz. This is the frequency band containing most of the energy of man-made noise produced in the area. The maximum contribution of man-made noise to the ambient noise environment was nearly 50 dB in this frequency band.

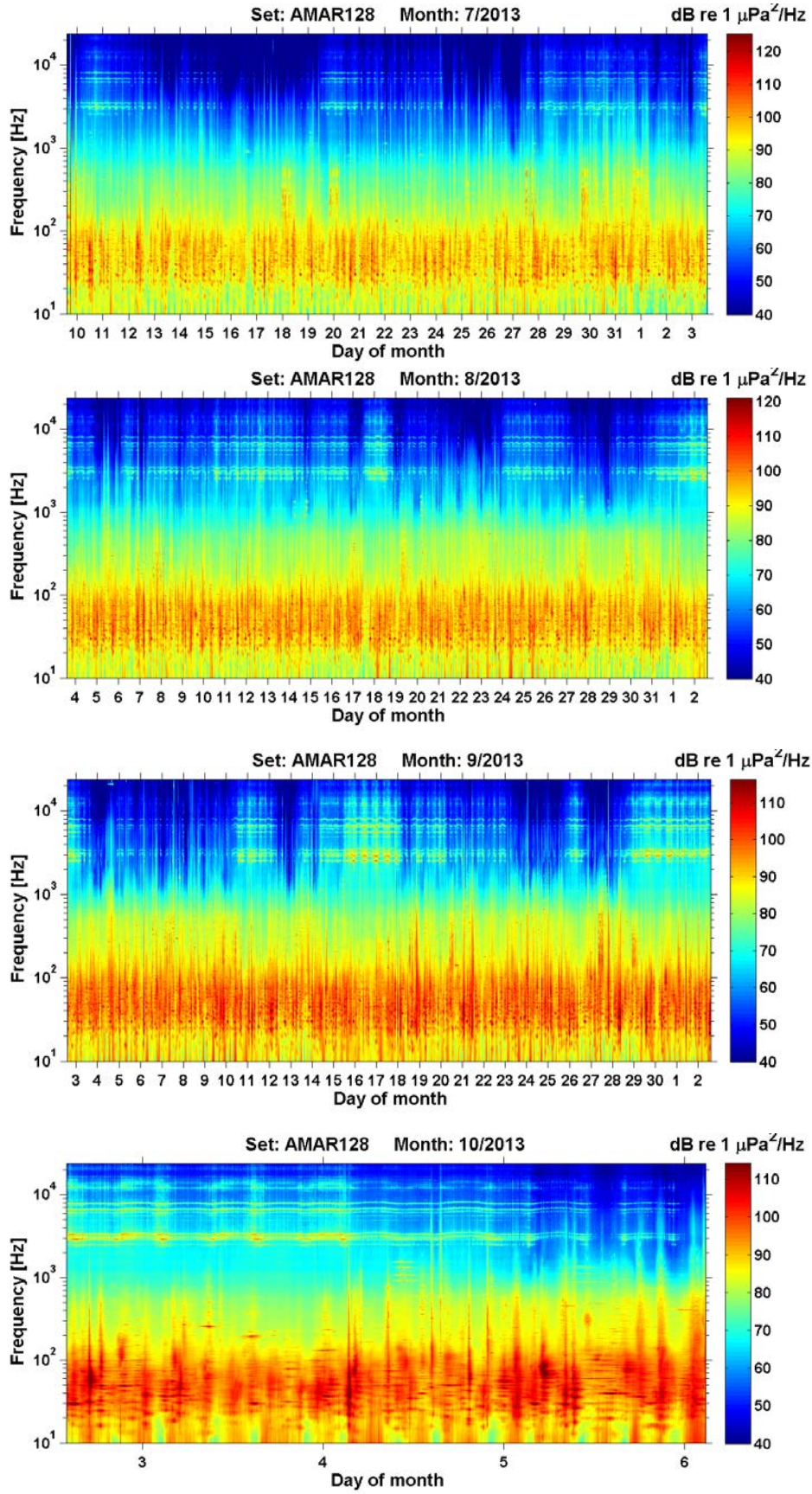


Figure 6: Frequency analysis of sound recorded per month at station GEMINI 1 (AMAR 128) (this page) and at station GEMINI 8 (AMAR 142) (next page) for July, August and September 2013. The power spectrum density (colour-coded, see legend on the right) is integrated over 5 min, displayed in dB re $1 \mu\text{Pa}^2/\text{Hz}$ and plotted as a function of frequency (in logarithmic units) over time.

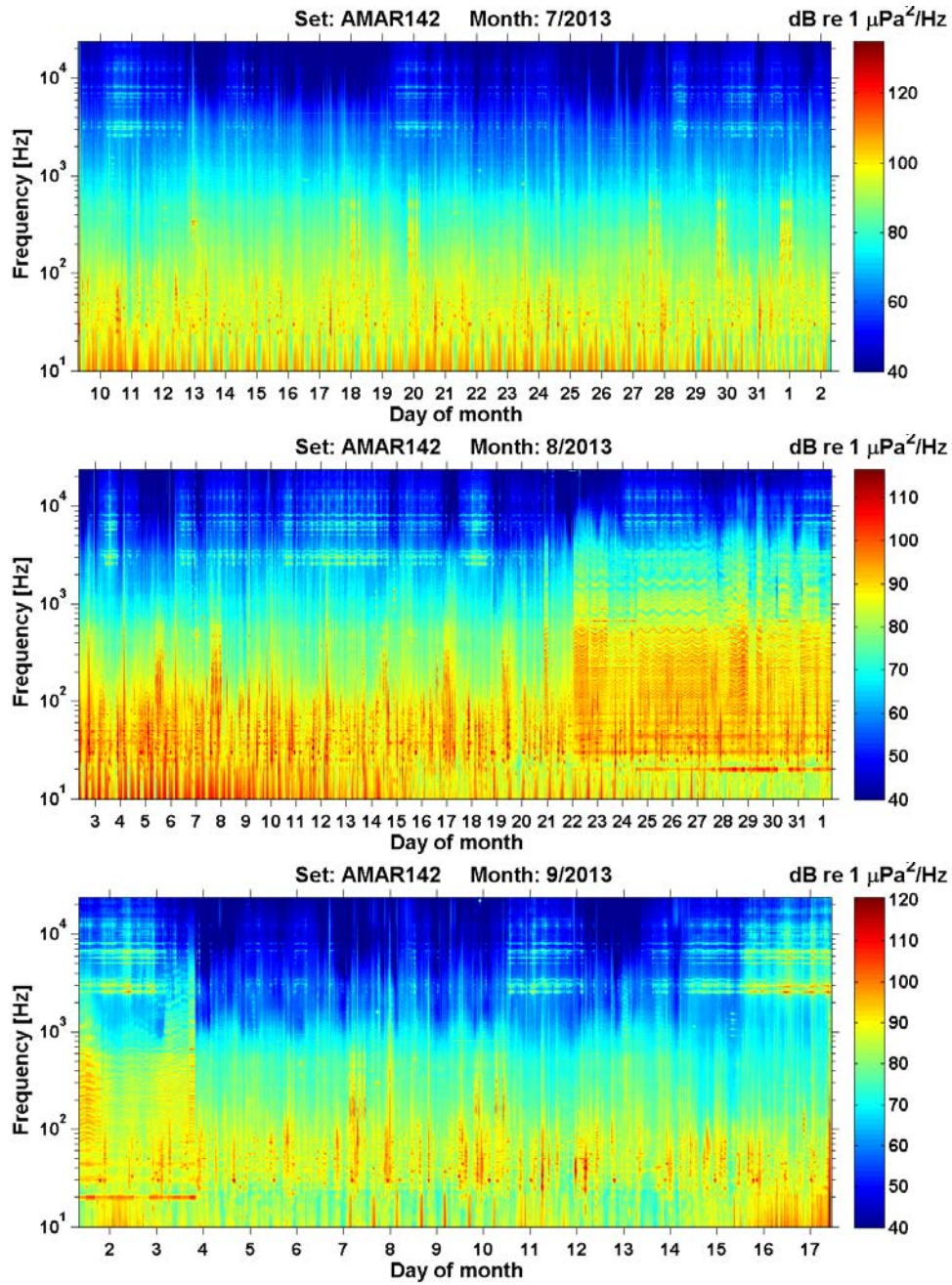


Figure 6: Continued – for AMAR 142, 2013.

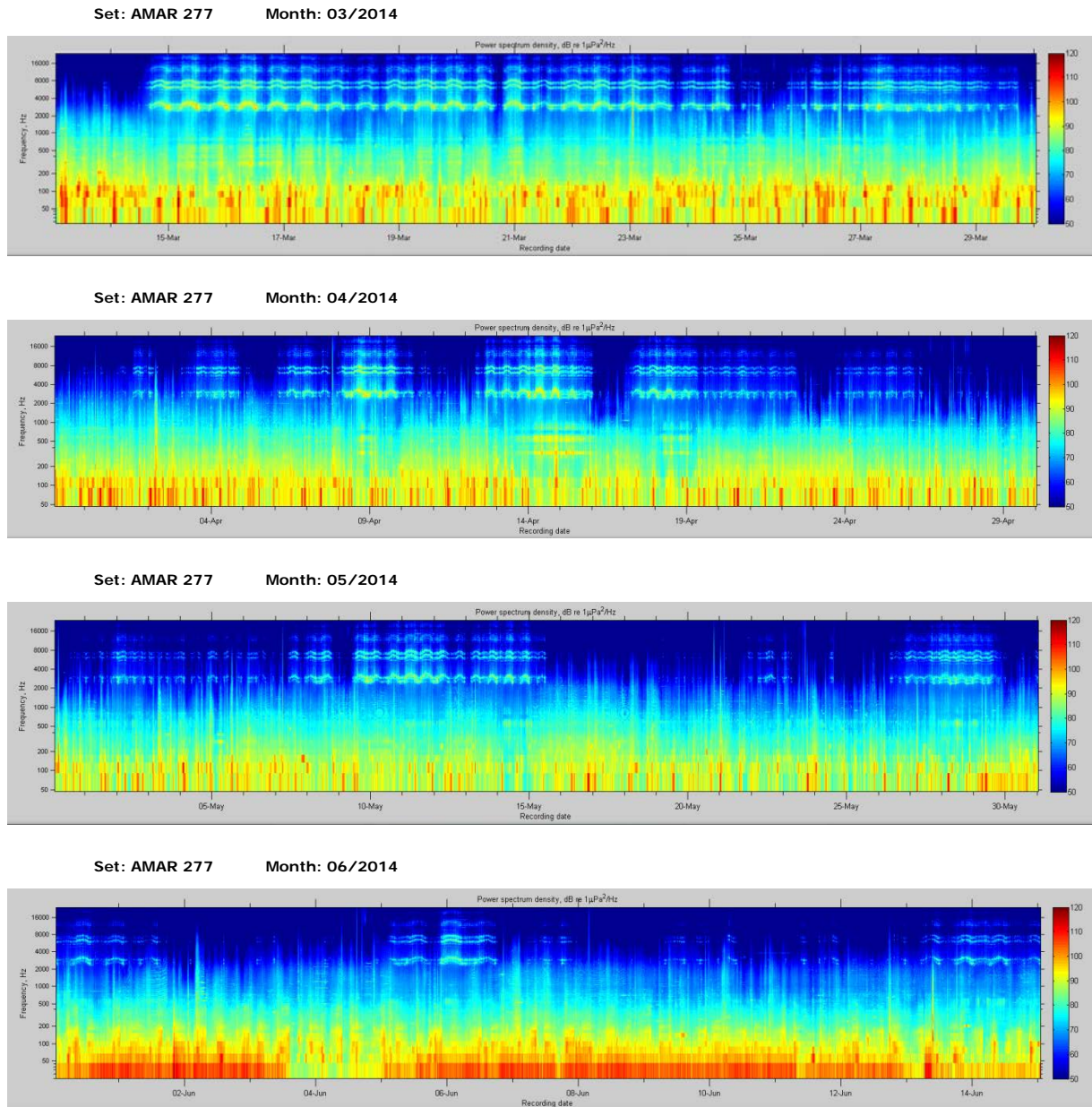
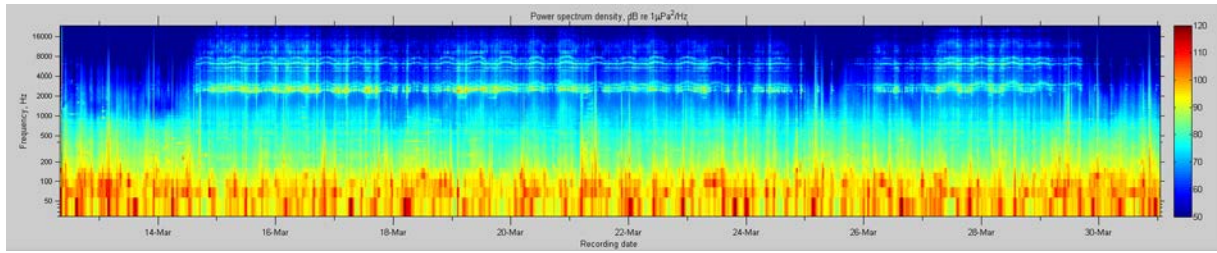


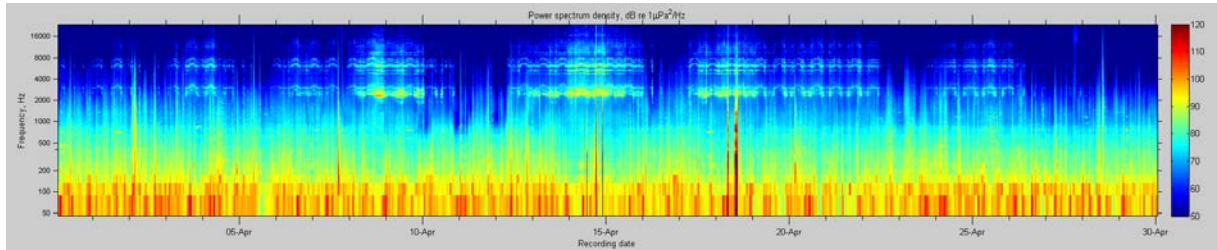
Figure 7: Frequency analysis of sound recorded per month at station GEMINI 1 (AMAR 277) for March- June 2014 (this page) and at station GEMINI 8 (AMAR 276) (next page) for March- July 2014 (note the difference in time scale for last plot, July 2014). The power spectrum density (colour-coded, see legend on the right) is integrated over 5 min, displayed in dB re $1\mu\text{Pa}^2/\text{Hz}$ and plotted as a function of frequency (in logarithmic units) over time.

Note that the recording of AMAR 277 at station GEMINI 1 ended on 15 June 2014. Over the following days the recorded sound level dropped consistently (down to zero; not shown in figure 7 and not included in the analysis) indicating an unexpected and premature loss of battery power.

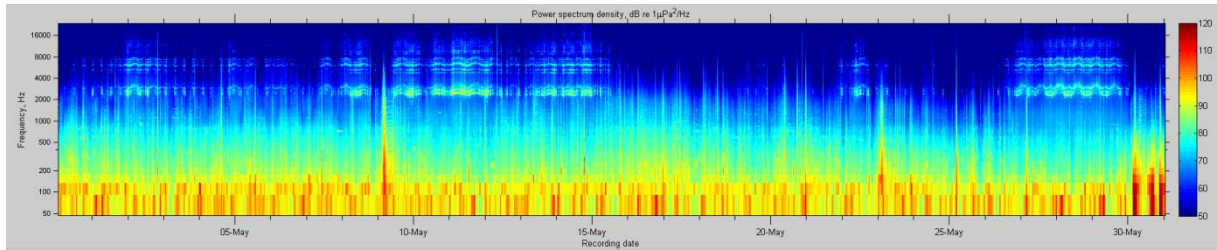
Set: AMAR 276 Month: 03/2014



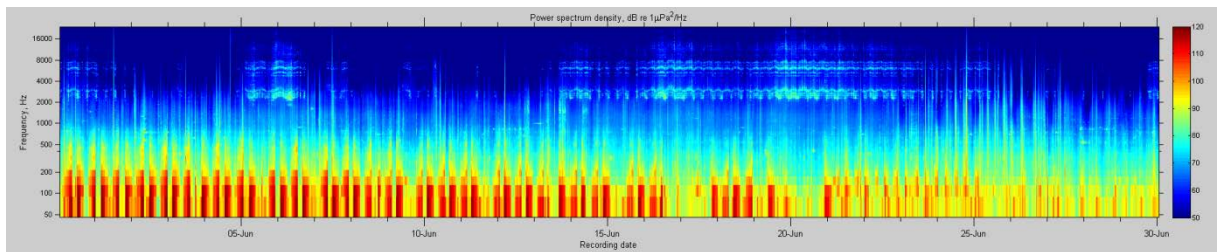
Set: AMAR 276 Month: 04/2014



Set: AMAR 276 Month: 05/2014



Set: AMAR 276 Month: 06/2014



Set: AMAR 276 Month: 07/2014

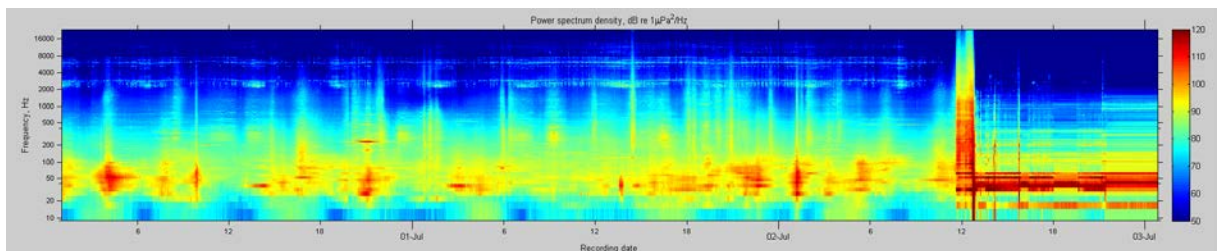


Figure 7: Continued – for AMAR 276, 2014.

Sound sources

1. Natural sound sources

Oceanographic and Meteorological

Increasing wind speeds would cause underwater sound by increased wave agitation. This is reflected in a raised overall background noise level. Other sources contributing to the natural background noise have not been identified within this study.

Current/ Flow noise

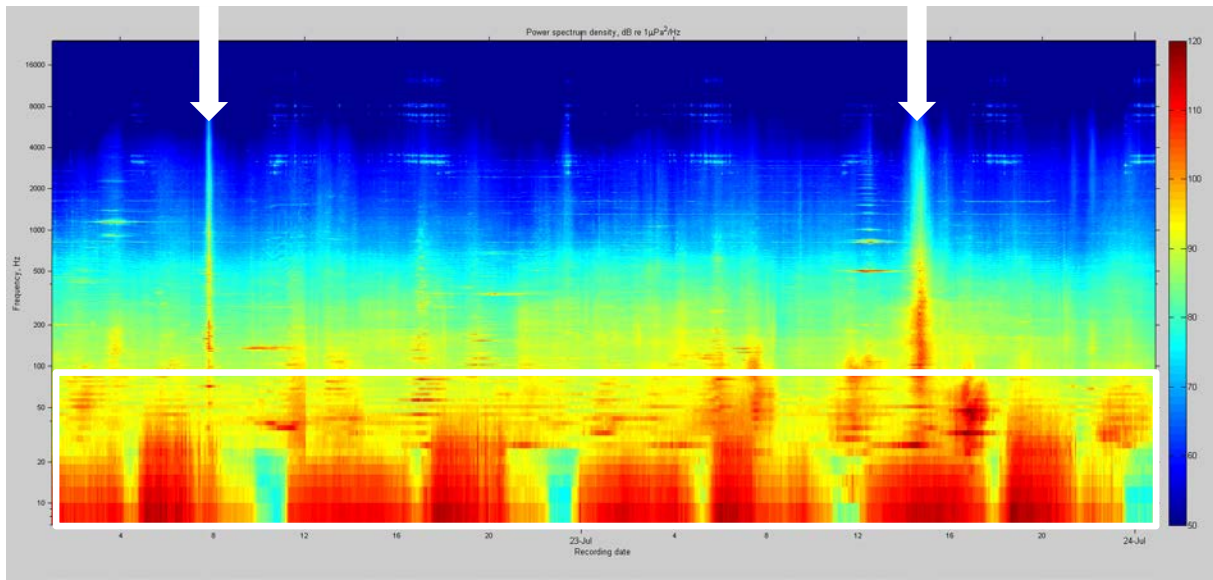


Figure 8: Frequency analysis of sound caused by tidal current (indicated by white box) and shipping activity (indicated by white arrows, see below: 2. Anthropogenic sounds). The power spectrum density (colour-coded, see legend on the right) is integrated over 5 min, displayed in dB re $1\mu\text{Pa}^2/\text{Hz}$ and plotted as a function of frequency (in logarithmic units) over time.

The tidal current can be identified by its low frequency content (usually below 100 Hz) and its repetitive occurrence (here lasting over several hours at a 12 hour interval). The sound is caused by water flowing along the hydrophone and has to be considered to be an artefact. The strength of the currents and consequently their acoustic signature changes seasonally.

Rainfall

Rain causes a continuous broadband sound underwater at low to moderate levels (Nystuen 1986), raising the ambient noise level by up to 20 dB in the recordings analysed (depending on the strength of the rain shower). The sound produced by rain covers a wide frequency and at low to moderate sound energy levels. However, due to its broadband nature it easily masks ('acoustically obscures') other signals (Figure 9).

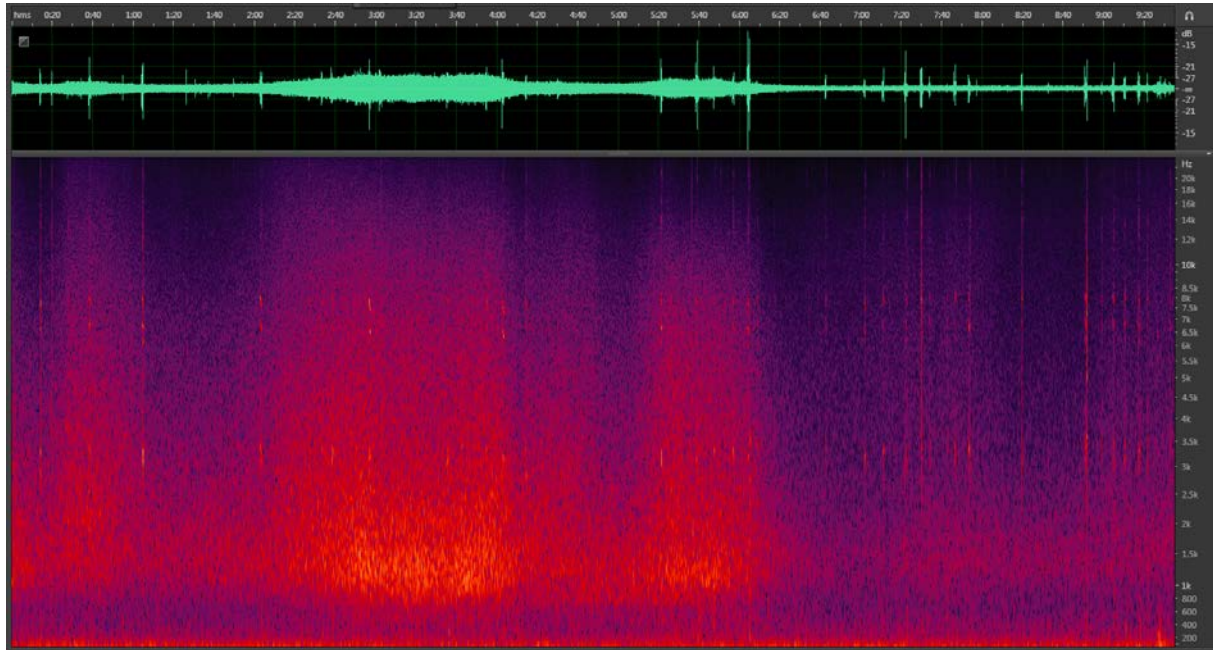


Figure 9: Frequency analysis of sound caused by rainfall. Time is displayed on the x-axis, the received level (in dB) on y-axis in the upper graph and frequency on a logarithmic scale (kHz) on the y-axis in the lower graph. The level of the received sound energy is colour coded in the lower graph (dark colour indicating low levels, bright colour indicating high levels with red as highest level).

Biological sounds

The only biological sounds identified from the recordings could represent the low frequency part of harbour porpoise echolocation signals (clicks, see Figure 10). The animals emit these signals for navigational purposes or to locate and identify objects such as food. Their frequency range stretches from <10 kHz to >160 kHz with most sound at levels between 110-150 kHz.

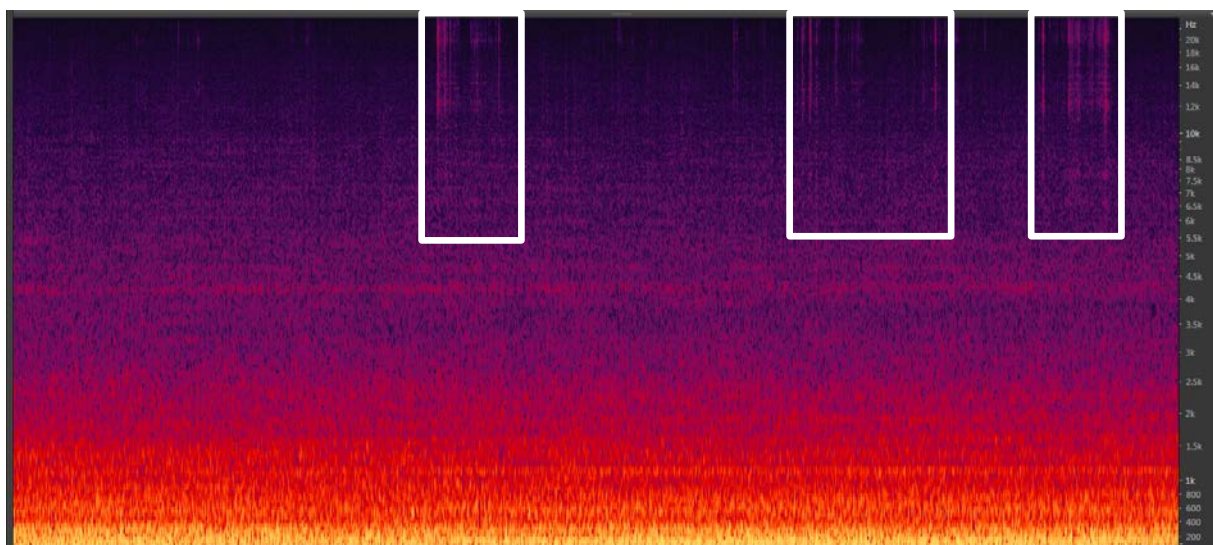


Figure 10: Frequency analysis possibly showing the low frequency end of porpoise clicks (indicated by white boxes). The level of the received sound energy is colour coded in the lower graph (dark colour indicating low levels, bright colour indicating high levels with red as highest level).

2. Anthropogenic sounds

Ship noise

Shipping activity was present in the recordings from both stations on every day over the entire study period (e.g. Figures 11, 12, 13). The acoustic energy of sound emitted by ships is concentrated at frequencies from <100 Hz to several 100 Hz. Additionally, ship sound is characterised by tonal components originating from machinery noise (Merchant et al. 2012). The sounds recorded at the two stations represent distant as well as nearby shipping activity. The distant shipping activity can mainly be attributed to large vessels using the main shipping routes at several (tens of) kilometres distance to the noise loggers. Due to their relatively high source level they are audible even over such a large distance, due to the frequency specific attenuation of the sound over large distances. They are not identifiable as individual ships but produce a constant low-to-mid frequency noise floor in the entire area. Nearby shipping sound most likely originates from trawlers passing by, either on their way to/from their fishing grounds, but in a few instances also busy trawling close to the noise loggers' positions. This nearby shipping activity can be discriminated by its spectral content and intensity. Close passages vary in duration, with longer durations (therefore slower speeds) indicating passages of trawlers with their nets down.

Shipping intensity differs between seasons; while distant shipping remained permanently present, shipping in the vicinity of the logger position was lower during spring (AMAR 227).

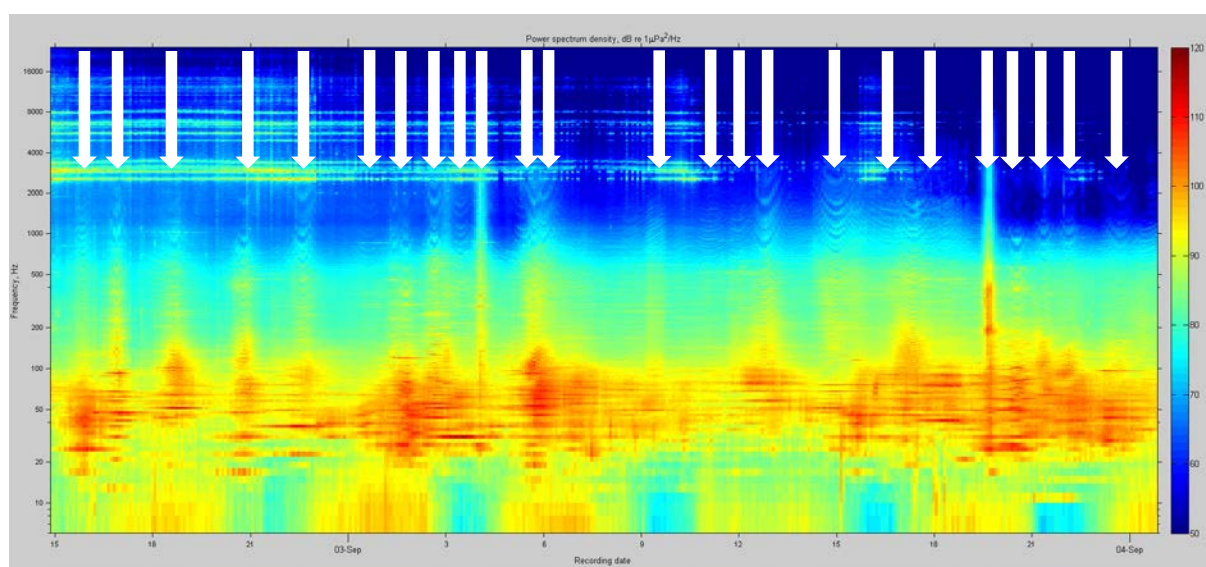


Figure 11: Frequency analysis of sound caused by shipping activity on 2 and 3 September 2013 recorded at position GEMINI 8; the white arrows indicate distinctive acoustic signature of individual ship passages. The power spectrum density (colour-coded, see legend on the right) is integrated over 5 min, displayed in dB re $1 \mu\text{Pa}^2/\text{Hz}$ and plotted as a function of frequency (in logarithmic units) over time. Over a period of 39 hours 24 ship passages were recorded.

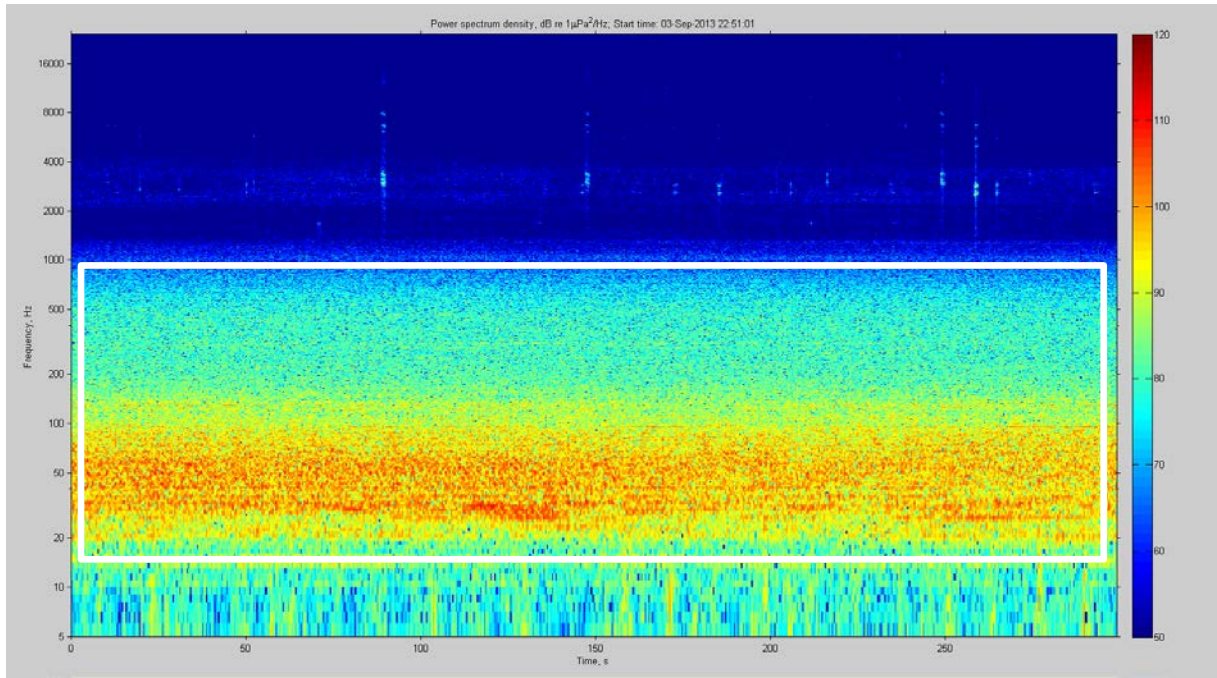


Figure 12: Frequency analysis of sound caused by low intensity shipping activity; the white box indicating the spectral range with the highest contribution from shipping sound. The power spectrum density (colour-coded, see legend on the right) is integrated over 1 s, displayed in dB re $1\mu\text{Pa}^2/\text{Hz}$ and plotted as a function of frequency (in logarithmic units) over time.

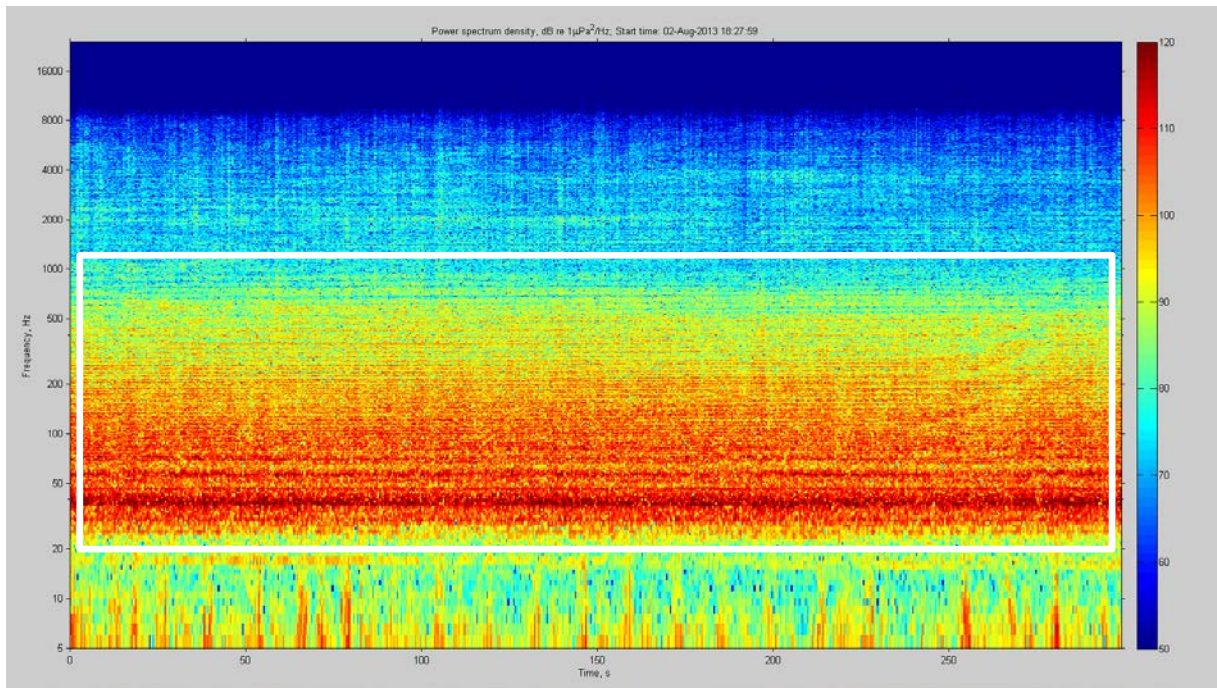


Figure 13: Frequency analysis of sound caused by high intensity shipping activity; the white box indicating the spectral range with the highest contribution from shipping sound. The power spectrum density (colour-coded, see legend on the right) is integrated over 1 s, displayed in dB re $1\mu\text{Pa}^2/\text{Hz}$ and plotted as a function of frequency (in logarithmic units) over time.

Echosounder

Almost all sea-going vessels use echosounder to probe the water depth or seek bathymetry. Fishing vessels use this technology in addition to find schools of fish and direct their course accordingly. Sound emissions from echosounders (usually catered at 38 kHz) are characterised by their repetitive, short and narrow-band 'pings' as can be seen at 20 kHz (the top of the frequency range, in white box) in Figure 14.

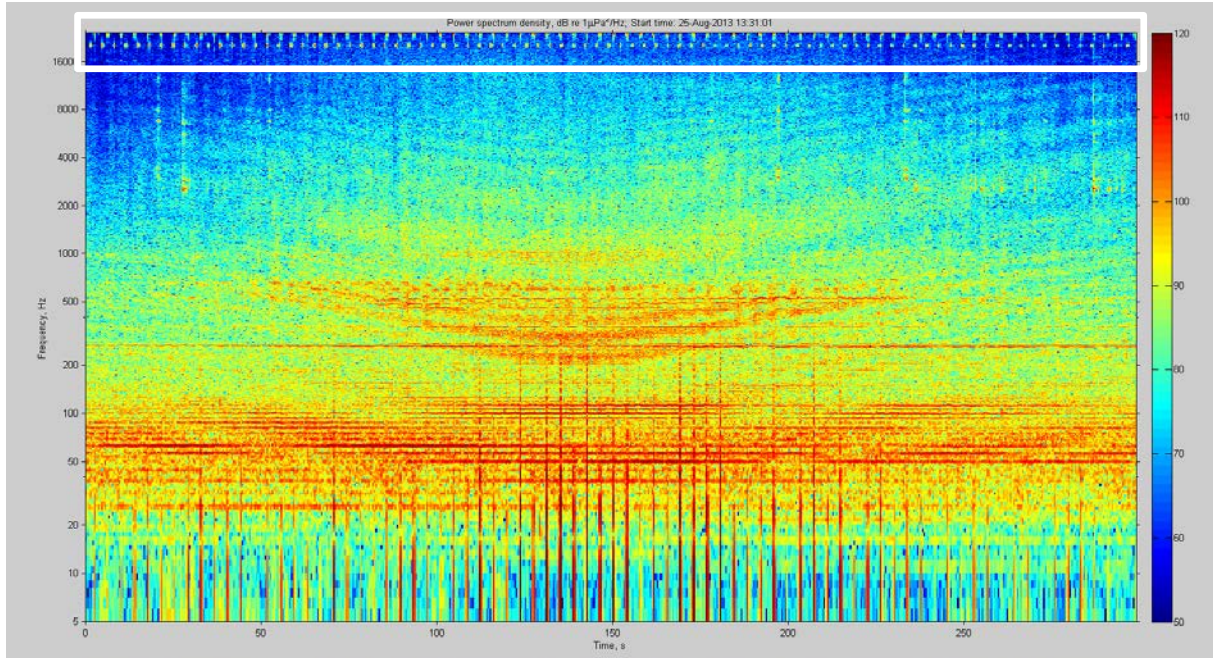


Figure 14: Frequency analysis of sound possibly caused by sonar (indicated by white box at 20 kHz; depth or fish finder) of ship passing-by at close distance. The power spectrum density (colour-coded, see legend on the right) is integrated over 1 s, displayed in dB re $1\mu\text{Pa}^2/\text{Hz}$ and plotted as a function of frequency (in logarithmic units) over time.

Pile driving

Acoustic emissions from pile driving into the marine sediment are highly repetitive, impulsive and broadband signals (see Figure 15, 16, 17). Due to their high source levels and high spectral energy at low frequencies, these signals can be detected over tens of kilometres.

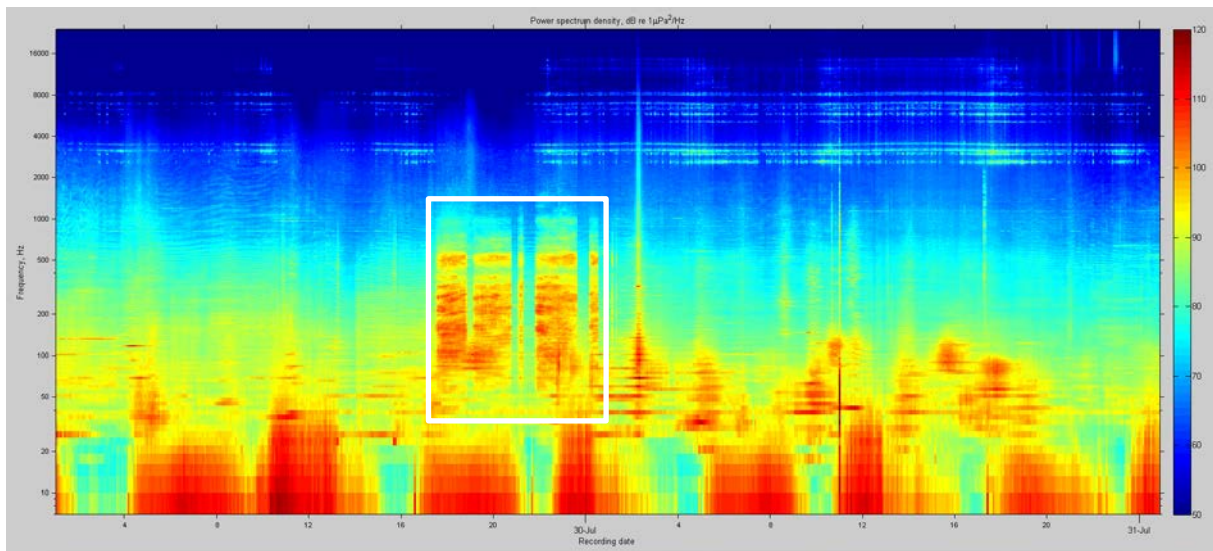


Figure 15: Frequency analysis of sound caused by distant pile driving recorded at station GEMINI 8 on 29 July 2013 between 17:30 and 23:35 UTC (indicated by white box). The power spectrum density (colour-coded, see legend on the right) is integrated over 5 min, displayed in dB re $1\mu\text{Pa}^2/\text{Hz}$ and plotted as a function of frequency (in logarithmic units) over time.

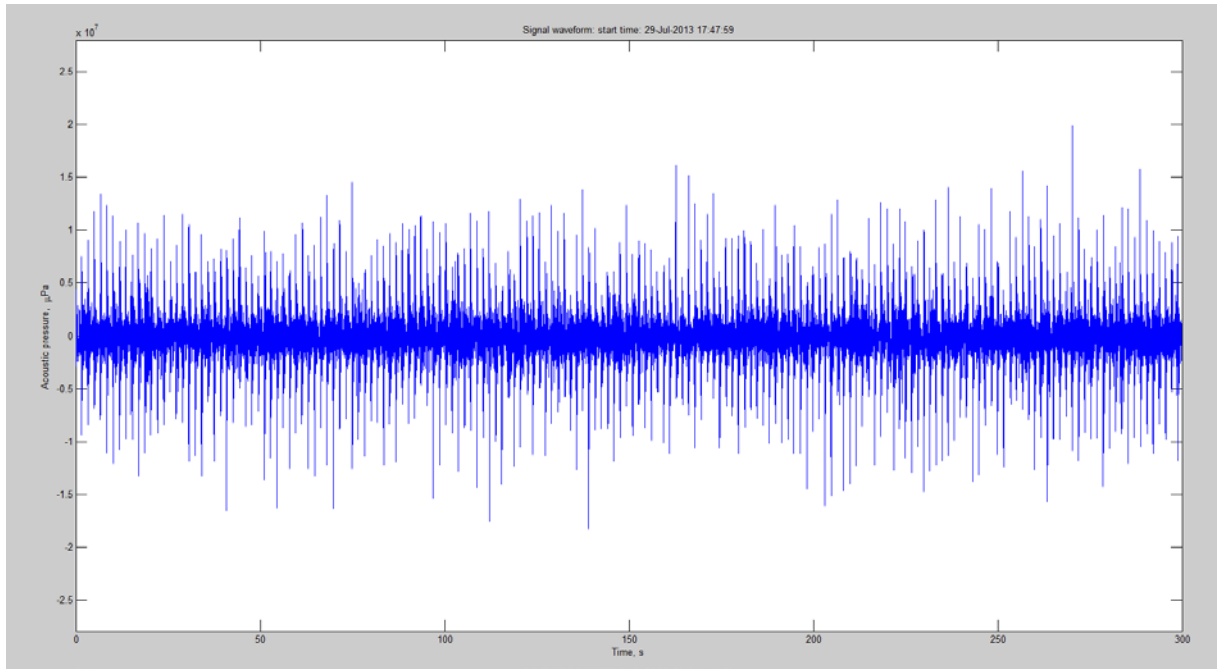


Figure 16: Waveform of sound received at station GEMINI 8 on 29 July 2013 and caused by distant pile driving. The acoustic pressure on the y-axis (in μPa) is plotted over time (seconds) on the x-axis.

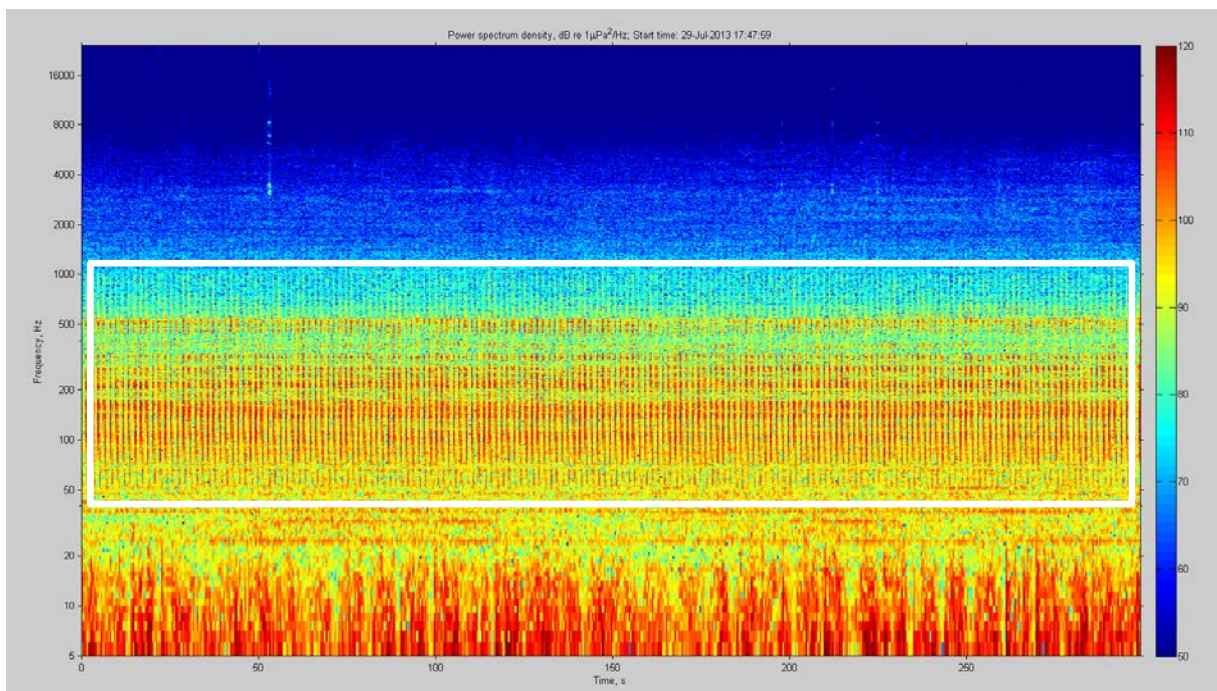


Figure 17: Frequency analysis of sound received at station GEMINI 8 on 29 July 2013 and caused by distant pile driving (indicated by white box). The power spectrum density (colour-coded, see legend on the right) is integrated over 1 s, displayed in dB re $1\mu\text{Pa}^2/\text{Hz}$ and plotted as a function of frequency (in logarithmic units) over time.

The difference in received acoustic energy between the two positions GEMINI 1 and 8 (with lower levels at position GEMINI 1 – not shown here – compared to GEMINI 8) indicates that the signals originate from pile driving activity in the German Bight. According to information on timing of construction activities for windparks in German/Danish waters (Luuk Folkerts, pers. comm., 04-09-2014) these signals possibly

originated from the windparks “Dan Tysk” or “Nordsee Ost”, both tens of kilometres from the noise logger positions.

Table 2. Timing information of pile driving activity identified on underwater sound recordings from position GEMINI 1 and 8 between July and September 2013. Several of the activities continued across days.

Date	Time	
	begin	end
18-07-2013	0200	0215
18-07-2013	0235	0500
18-07-2013	0530	0533
18-07-2013	0625	0815
18-07-2013	0835	0836
18-07-2013	0903	0920
19-07-2013	2316	
20-07-2013		0057
20-07-2013	0123	0148
20-07-2013	0243	0433
20-07-2013	0539	0615
20-07-2013	0641	0651
27-07-2013	1248	1358
27-07-2013	1411	1428
27-07-2013	1521	1554
27-07-2013	1828	2005
27-07-2013	2018	2029
27-07-2013	2139	2227
29-07-2013	1730	1850
29-07-2013	1900	2045
29-07-2013	2105	2115
29-07-2013	2150	2335
30-07-2013	0010	0145
31-07-2013	1730	1940
31-07-2013	1945	2020
31-07-2013	2030	2045
31-07-2013	2100	2240
31-07-2013	2245	2320
31-07-2013	2340	2345
01-08-2013	0000	0230
05-08-2013	0945	1010
05-08-2013	1020	1130
05-08-2013	1140	1400
05-08-2013	1415	1600
05-08-2013	1630	1800
07-08-2013	1550	1845
07-08-2013	1915	2157
07-08-2013	2319	

08-08-2013		0148
14-08-2013	0900	1015
Date	Time	
	begin	end
14-08-2013	1130	1200
14-08-2013	1210	1315
14-08-2013	1430	1545
16-08-2013	1420	1520
16-08-2013	1550	1610
16-08-2013	2150	2300
16-08-2013	2350	
17-08-2013		0045
17-08-2013	0215	0300
19-08-2013	0600	0655
19-08-2013	0710	0800
19-08-2013	0820	1000
19-08-2013	1045	1135
19-08-2013	1230	1325
19-08-2013	1335	1340
20-08-2013	2230	
21-08-2013		0145
07-09-2013	0400	0500
07-09-2013	0530	0720
07-09-2013	0845	1015
07-09-2013	1130	1230

Pile driving impulses were detected on 18 days between 18-07-2013 and 07-09-2013 over a total of 62 hours. Due to their transient nature, lasting less than half a second at a repetition rate of two seconds on average (i.e. with a duty cycle of 25%), the pile driving impulses were acoustically present over a total of approximately 15.5 hours.

A second sequence of pile driving events was detected in the recordings from 2014.

Table 3. Timing information of pile driving activity identified on underwater sound recordings from position GEMINI 1 and 8 between April and June 2014. Several of the activities continued across days.

Date	Time	
	begin	end
25-04-2014	0834	0906
25-04-2014	0931	1000
25-04-2014	1022	1029
25-04-2014	1049	1125
25-04-2014	1142	1150
25-04-2014	1210	1300
25-04-2014	1322	1442
25-04-2014	1506	1628
25-04-2014	1928	2010

25-04-2014	2047	2127
25-04-2014	2141	2232
Date	Time	
	begin	end
01-05-2014	0000	0118
01-05-2014	0142	0222
01-05-2014	0548	0632
01-05-2014	0659	0740
01-05-2014	0800	0905
01-05-2014	2246	2332
02-05-2014	0142	0232
02-05-2014	0257	0412
29-05-2014	2000	2205
29-05-2014	2205	2218
29-05-2014	2218	2232
29-05-2014	2232	2250
30-05-2014	0313	0805
30-05-2014	1245	1733
30-05-2014	2045	
31-05-2014		0130
31-05-2014	1215	1700
31-05-2014	1955	
01-06-2014		0030
01-06-2014	0355	0850
01-06-2014	1130	1610
01-06-2014	1955	
02-06-2014		0037
02-06-2014	0310	0805
02-06-2014	1135	1617
02-06-2014	1900	2340
03-06-2014	0240	0723
03-06-2014	0950	1430
03-06-2014	1745	1820
03-06-2014	2150	
04-06-2014		0230
04-06-2014	0500	0945
04-06-2014	1250	1730
04-06-2014	2050	
05-06-2014		0130
05-06-2014	0500	0945
05-06-2014	1300	1350
05-06-2014	1750	2215
06-06-2014	0115	0610
06-06-2014	0810	1245
06-06-2014	1550	2030
07-06-2014	0405	0835

07-06-2014	1130	1610
07-06-2014	1730	2230
Date	Time	
	begin	end
08-06-2014	0105	0600
08-06-2014	0840	1320
08-06-2014	1720	1920
08-06-2014	2200	
09-06-2014		0230
09-06-2014	0515	1000
09-06-2014	1830	2300
10-06-2014	0125	0610
10-06-2014	0900	1330
10-06-2014	1600	2040
10-06-2014	2300	
11-06-2014		0350
11-06-2014	0630	1100
11-06-2014	2045	
12-06-2014		0130
12-06-2014	0350	0830
12-06-2014	1100	1530
12-06-2014	1815	2300
13-06-2014	0130	0610
13-06-2014	1545	2015
13-06-2014	2315	
14-06-2014		0400
14-06-2014	0630	0930
14-06-2014	1315	1750
14-06-2014	2040	
15-06-2014		0125
15-06-2014	1200	1700
15-06-2014	1930	
16-06-2014		0020
16-06-2014	0300	0750
16-06-2014	1040	1215
17-06-2014	1945	2400
18-06-2014	0245	0725
18-06-2014	0950	1440
18-06-2014	1800	2245
19-06-2014	0825	1330
20-06-2014	2140	
21-06-2014		0240
21-06-2014	0530	0800
21-06-2014	1125	1415
21-06-2014	1730	2015

22-06-2014	0000	0250
22-06-2014	0645	0900
22-06-2014	1310	1600
Date	Time	
	begin	end
22-06-2014	1900	2200
23-06-2014	0220	0530
23-06-2014	0800	1100
23-06-2014	1545	1830
23-06-2014	2200	
24-06-2014		0015
24-06-2014	0445	0745
24-06-2014	1100	1330
24-06-2014	1745	2040
25-06-2014	0000	0300

In 2014, pile driving impulses were detected at relatively low received levels (i.e. from a more distant source) between 25-04-2014 and 02-05-2014 over periods of approximately 15 hours at a rate of 1.7 impulses per second. On 29-05-2014 a soft start period with varying impulse intervals and received levels was recorded between 2200 and 2250. Between 30-05-2014 and 25-06-2014 pile driving impulses were detected in the recordings at high received levels (up to 130-140 dB re 1 μ Pa) over a total period of >311 hours. These pile driving impulses were at a lower rate, with five seconds between successive impulses.

Explosions

Underwater explosions to clear Second World-War unexploded ordnance, such as aerial bombs, ammunition, mines and torpedoes occur often in the southern North Sea, compared with other marine areas. Exploding high-order ordnance produces an overpressure shock wave which is transmitted through the water, as well as the ground. At greater distances the low-frequency ground wave gradually re-enters the water column, but – due to a faster propagation in the denser ground – precedes the shock wave transmitted through the water. An underwater explosion can be characterised by the initial low-frequency component (transmitted through the sea-floor), followed by a short broadband signal with a sharp rise-time (creating a distinct onset with a sharp contrast in the spectrogram, see Figures 18-21).

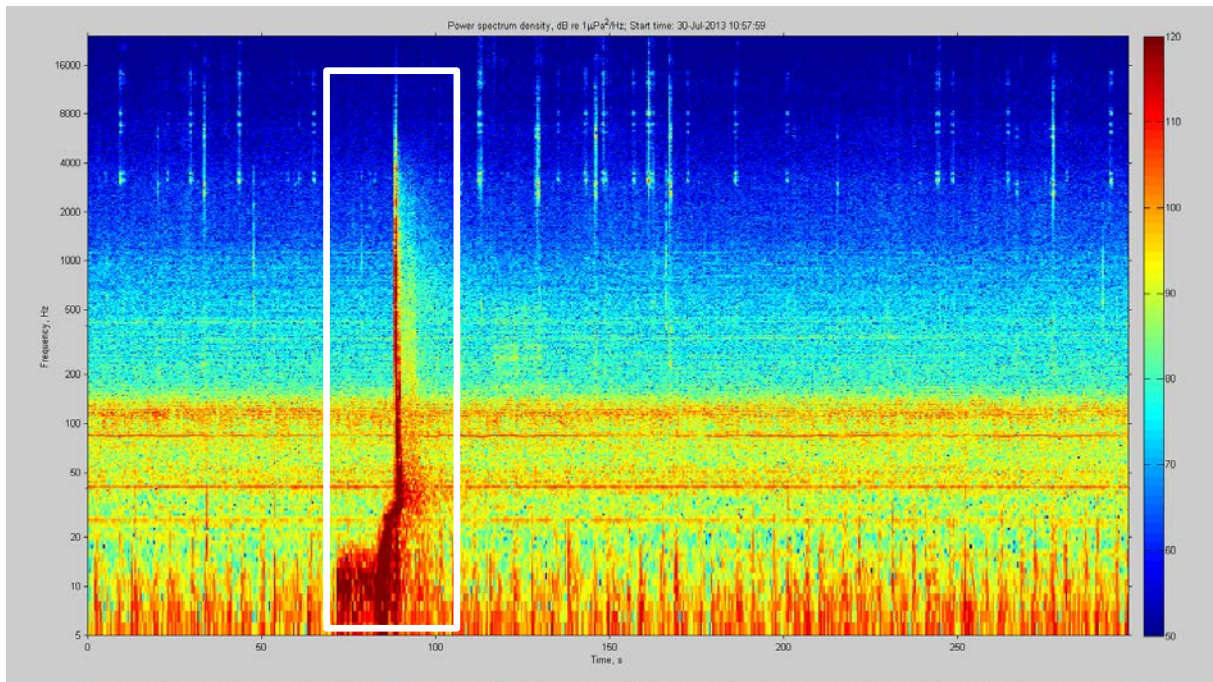


Figure 18: Frequency analysis of sound at station GEMINI 8 on 30 July 2013 at 11:00 UTC caused by a distant underwater explosion (indicated by white box). The power spectrum density (colour-coded, see legend on the right) is integrated over 1 s, displayed in dB re $1\mu\text{Pa}^2/\text{Hz}$ and plotted as a function of frequency (in logarithmic units) over time.

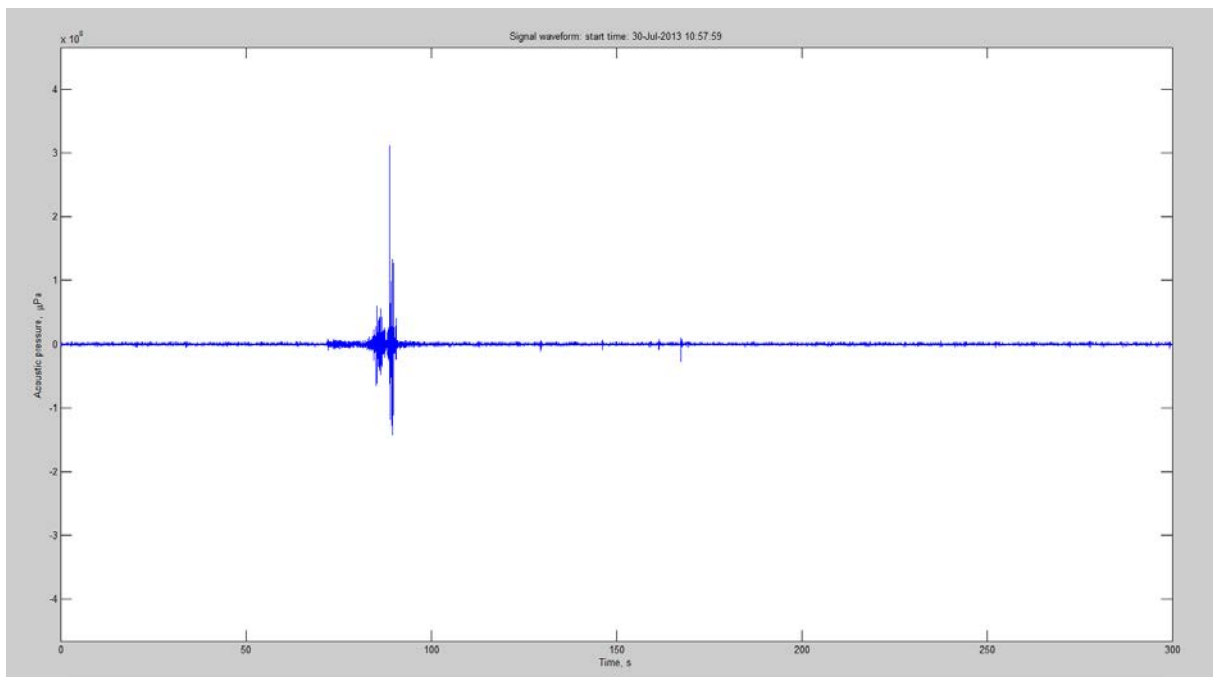


Figure 19: Waveform of sound at station GEMINI 8 on 30 July 2013 at 11:00 UTC caused by a distant underwater explosion. The acoustic pressure on the y-axis (in μPa) is plotted over time (seconds) on the x-axis.

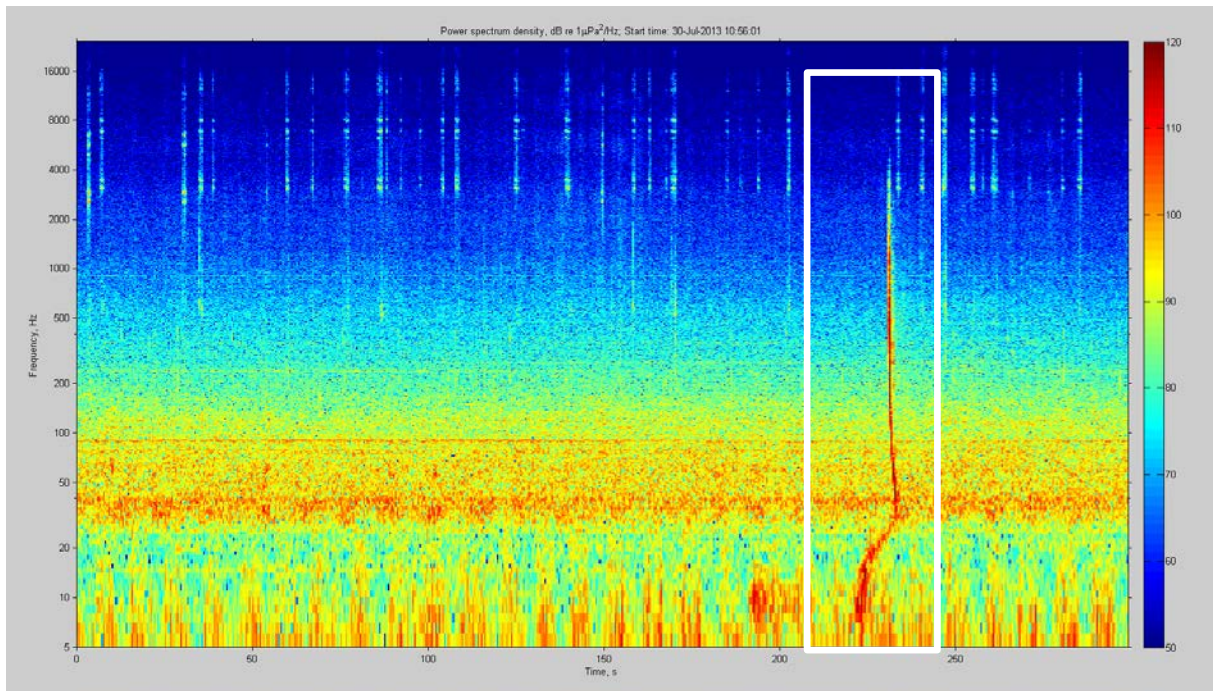


Figure 20: Frequency analysis of sound recorded at station GEMINI 1 on 30 July 2013 at 11:00 UTC caused by the same distant underwater explosion (indicated by white box) as shown in Figure 18. The power spectrum density (colour-coded, see legend on the right) is integrated over 1 s, displayed in dB re $1\mu\text{Pa}^2/\text{Hz}$ and plotted as a function of frequency (in logarithmic units) over time.

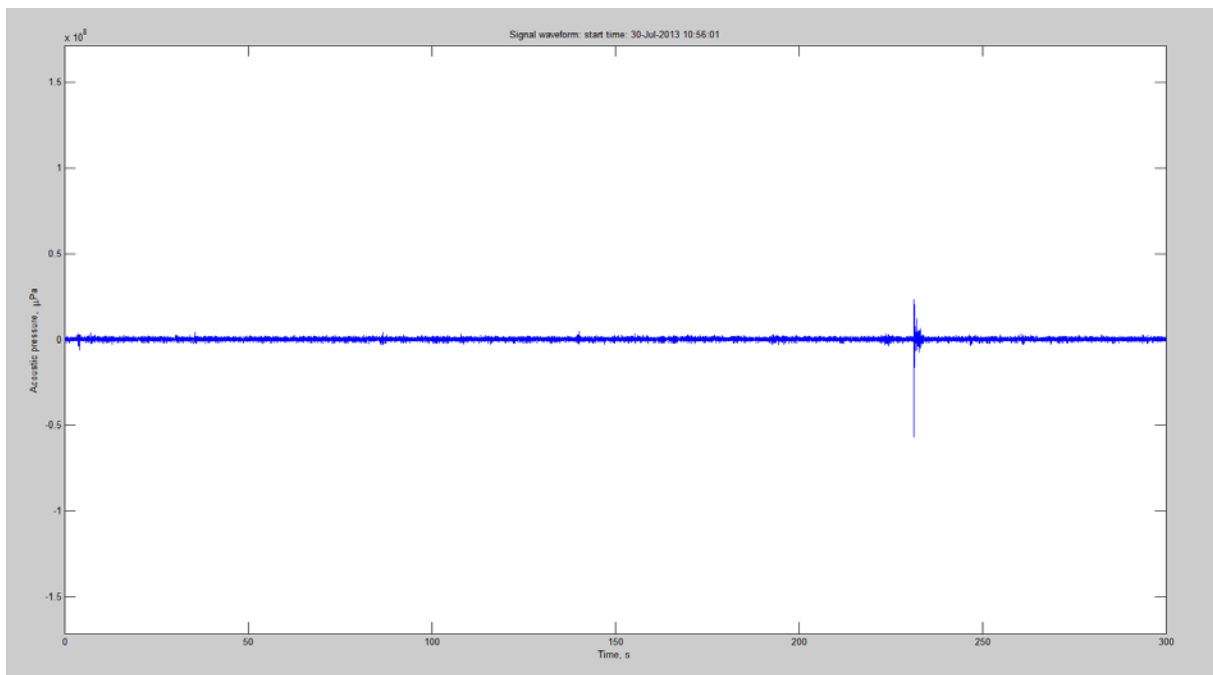


Figure 21: Waveform of sound recorded at station GEMINI 1 on 30 July 2013 at 11:00 UTC caused by the same distant underwater explosion as shown in figure 19.

The difference in acoustic energy as well as a difference in the time of recording of the acoustic signature of this explosion at two stations which were 40 km apart allows tracing the position of the explosion back into German waters. The difference in received amplitude and energy corresponds to more westerly direction, i.e. the explosion occurred most likely in the southern part of the German Bight. It would have been audible and detectable above ambient noise over a much wider distance from the source than the two noise loggers. Three more explosions were clearly identified in the recordings and two more acoustic events could potentially also be attributed to such explosions (Table 4).

Table 4: List of underwater explosions detected in recordings at position GEMINI 1 and 8 between July and September 2013.

Date [yyyy]	Time [hhmm]	Activity explosion	Comment
30-07-2013	1058	near, >120 dB	confirmed
30-07-2013	1719	distant	uncertain
31-07-2013	1610	distant	uncertain
31-07-2013	2004	distant	confirmed
02-08-2013	1722	distant	confirmed
02-08-2013	1807	near, >120 dB	confirmed

Mooring – Station Self Noise

The mooring chain of the buoys used to anchor the noise loggers at their positions consists of steel links. When the surface buoys are agitated by wave motion, the chains begin to move accordingly, which creates a transient, broadband sound. Its source level is low compared to most other sounds recorded and detected in these recordings. Due to its direct proximity the source level, nevertheless, is recorded at almost equivalent levels to some of the distant sounds. The rattling sound of the chains would likely be audible above ambient noise over a distance of approximately 100 meters. In Figure 22 several bursts of chain noise can be identified, most likely representing periods of wave-agitated buoy movements.

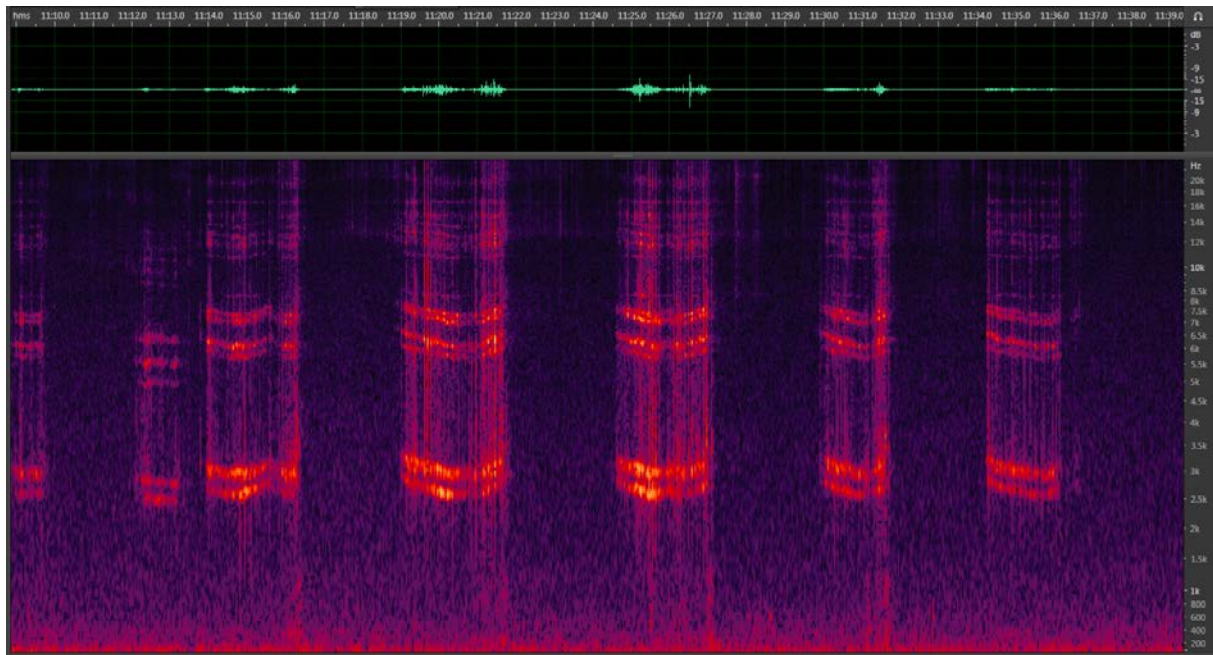


Figure 22: Frequency analysis of sound caused by anchor chains. Time is displayed on the x-axis, the received level on a logarithmic scale (dB) on y-axis in the upper graph and frequency on a logarithmic scale (kHz) on the y-axis in the lower graph. The level of the received sound energy is colour coded in the lower graph (dark colour indicating low levels, bright colour indicating high levels with yellow as highest level).

Mooring – unidentified sound source

On several occasions in 2014 objects touching the metal case protecting the hydrophone caused broadband sounds at relatively high received levels (see Figures 23–25). Since these sounds were caused in direct contact or in the vicinity of the receiving hydrophone, they should be considered as artefacts. It is unclear whether the objects touching the noise recorder were of biological nature (fish, benthic animals etc.) or anthropogenic origin (fishing nets, ropes etc. temporarily entangled in the noise logger). These acoustic artefacts occurred repeatedly on 14 and 18 April as well as on 15 May 2014.

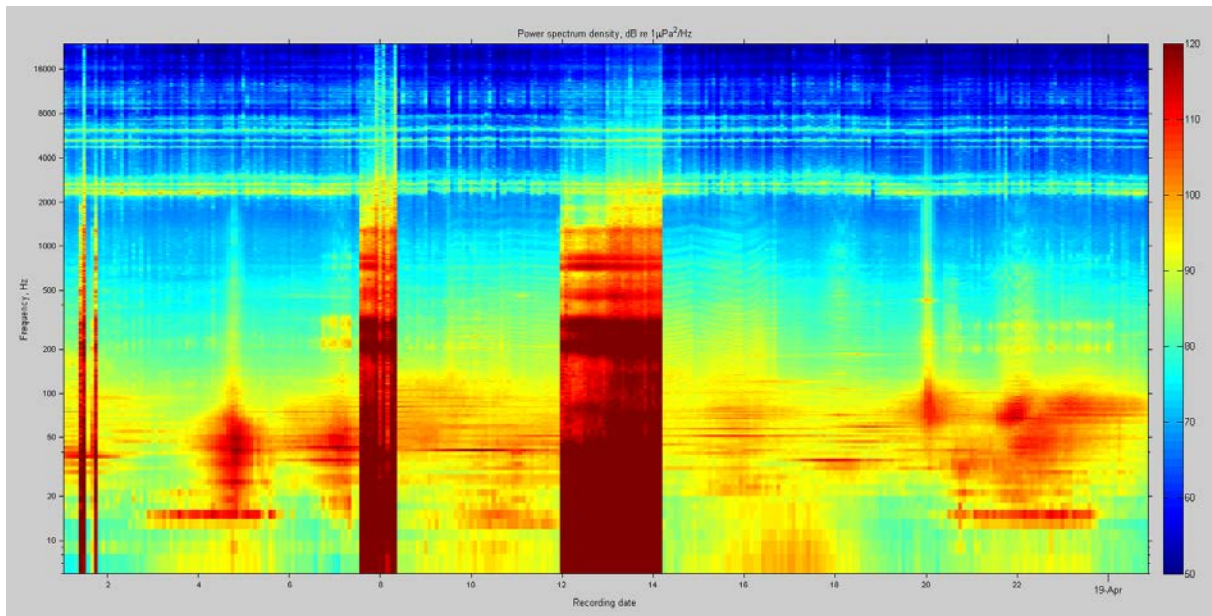


Figure 23: Frequency analysis of sound caused by unknown objects touching the noise logger. Time is displayed in hours on the x-axis, the received level on a logarithmic scale (dB) on y-axis in the upper graph and frequency on a logarithmic scale (kHz) on the y-axis in the lower graph. The power spectrum density (colour-coded, see legend on the right) is integrated over 5 min, displayed in dB re 1μPa²/Hz and plotted as a function of frequency (in logarithmic units) over time.

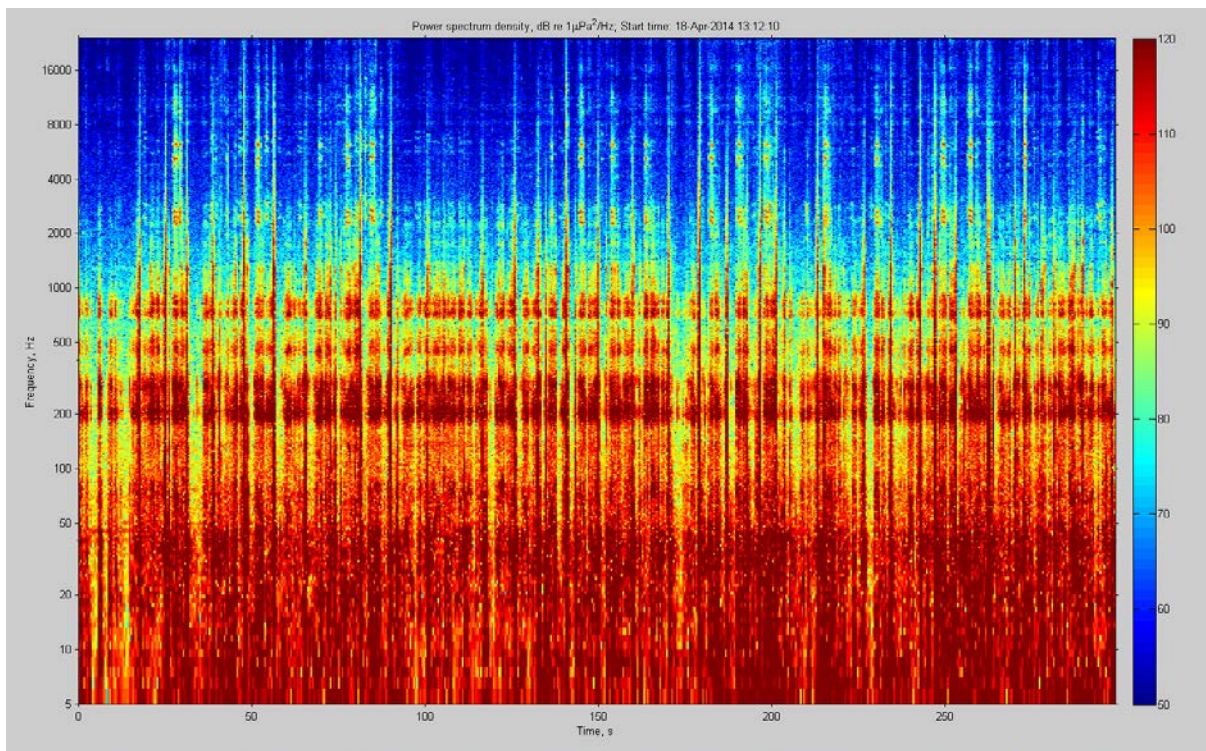


Figure 24: Frequency analysis of sound caused by unknown objects touching the noise logger at higher temporal resolution compared to Figure 23. The sequence shown in this figure begins at 13:12:10. Time is displayed in seconds on the x-axis, the received level on a logarithmic scale (dB) on y-axis in the upper graph and frequency on a logarithmic scale (kHz) on the y-axis in the lower graph. The power spectrum density (colour-coded, see legend on the right) is integrated over 1 s, displayed in dB re 1 $\mu\text{Pa}^2/\text{Hz}$ and plotted as a function of frequency (in logarithmic units) over time.

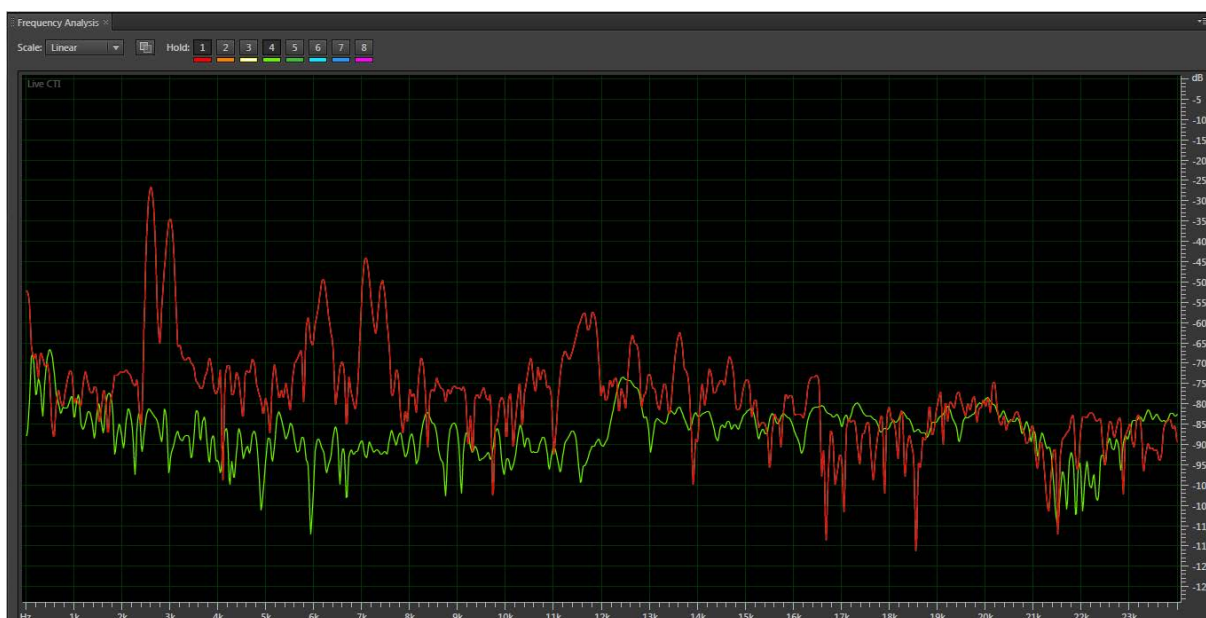


Figure 25: Frequency analysis of sound caused by anchor chains at station GEMINI 8 (red line) relative to background noise at the same position (green line). Frequency (kHz, in linear units) is displayed on the x-axis and the spectral energy content of the acoustic signal (in dB) on the y-axis.

Combined sounds

On average, the soundscape at both noise logger positions was composed of a variety of different sounds occurring at the same time. If the spectral contents of the sounds overlap they can mask each other, which makes it difficult to identify the individual sound sources (e.g. Figure 26). At the same time, such overlap in time and spectral content leads to an increase in sound energy at the particular moment and frequencies.

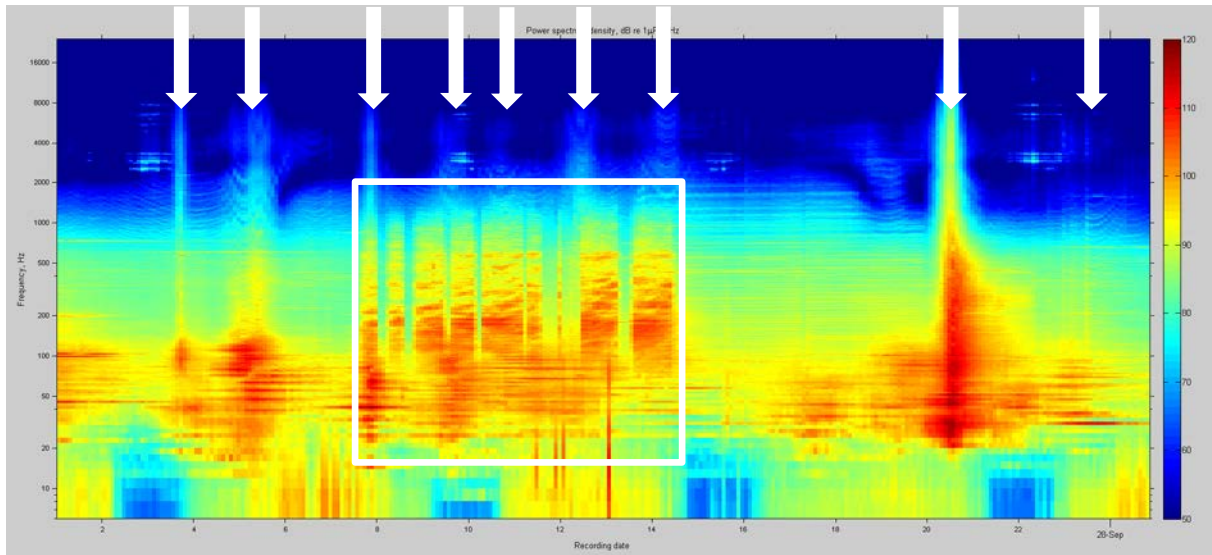


Figure 26: Frequency analysis of sound caused by pile driving (several periods within white box) and shipping (indicated by white arrows). The power spectrum density (colour-coded, see legend on the right) is integrated over 5 min, displayed in dB re $1\mu\text{Pa}^2/\text{Hz}$ and plotted as a function of frequency (in logarithmic units) over time.

Unidentified

Several sounds were visually detected, but could not be identified – neither based on their acoustic signatures nor by auditory analysis through an acoustic expert (Figures 27-29). However, several windpark related activities were conducted by Fugro (Luuk Folkerts, pers. comm.) in 2011-2014. These activities include boreholes, cone penetration tests, and side scan sonar and magnetometer measurements. One of the activities was identified in the recordings (see 'Results', page 13). It is unclear if and to what extent the other activities may have been contributing to the acoustic scene in the study and if one of the unidentified sounds displayed in the graphs below can be correlated to them.

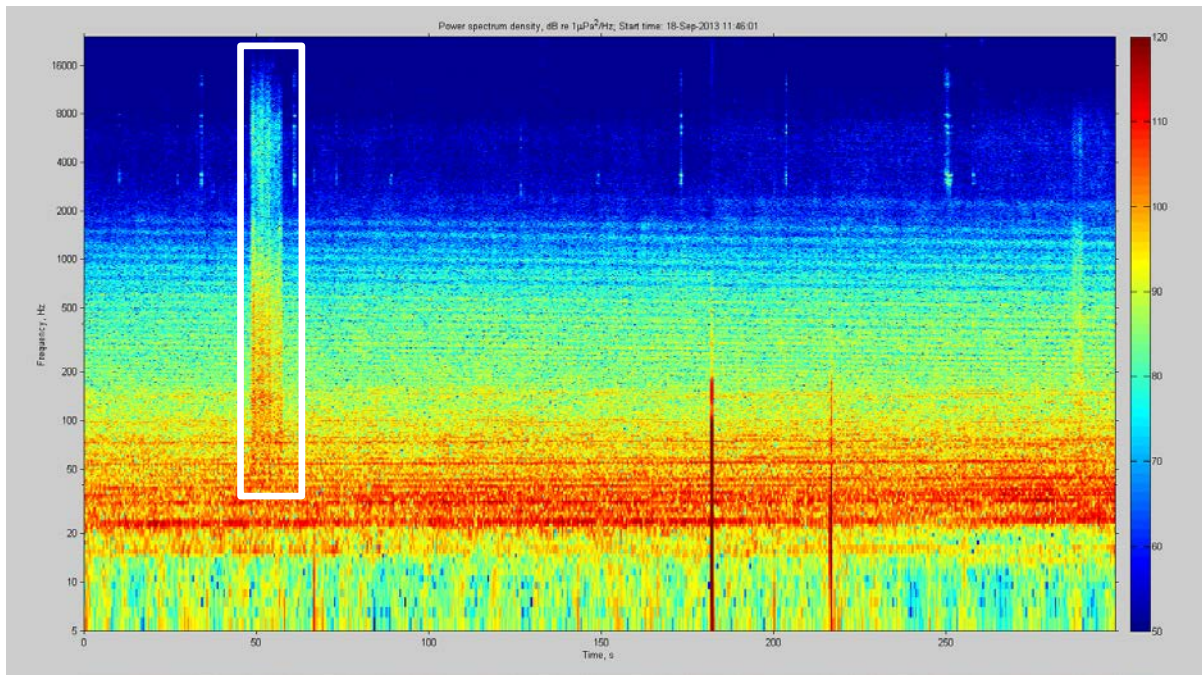


Figure 27: Frequency analysis of unidentified sound (white box) recorded on 18 September 2013. The power spectrum density (colour-coded, see legend on the right) is integrated over 1 s, displayed in dB re $1 \mu\text{Pa}^2/\text{Hz}$ and plotted as a function of frequency (in logarithmic units) over time (The dark vertical lines are system artefacts).

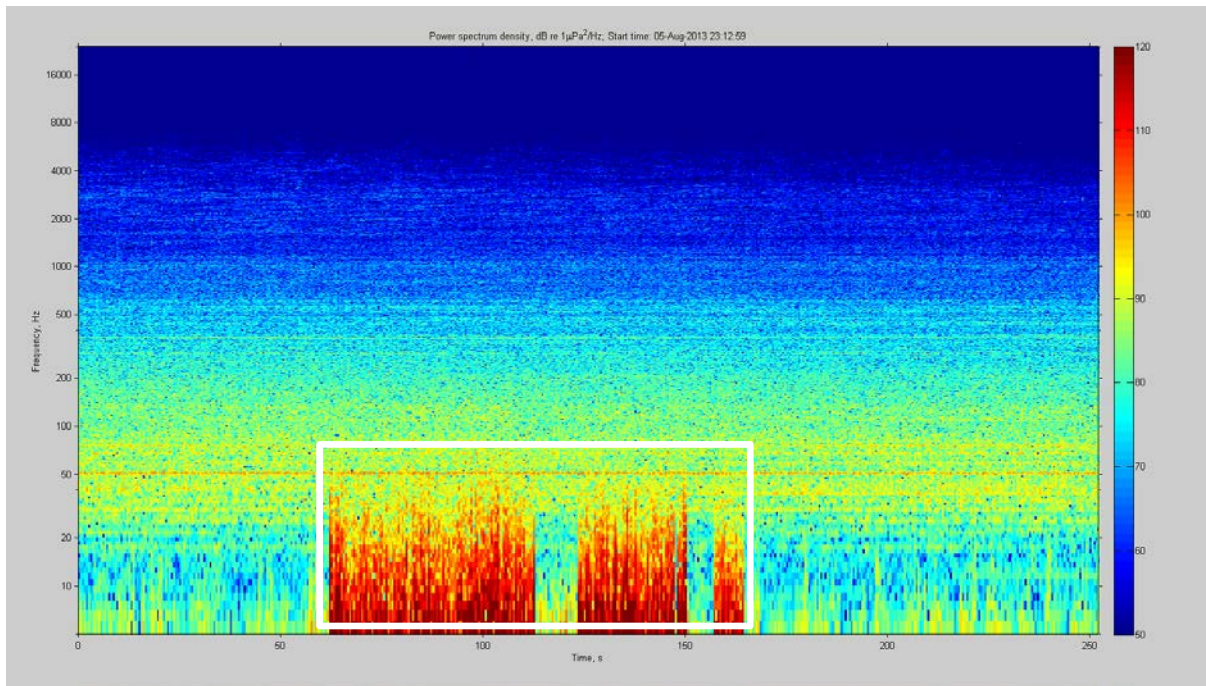


Figure 28: Frequency analysis of unidentified sound (white box) recorded on 5 August 2013. The power spectrum density (colour-coded, see legend on the right) is integrated over 1 s, displayed in dB re $1\mu\text{Pa}^2/\text{Hz}$ and plotted as a function of frequency (in logarithmic units) over time.

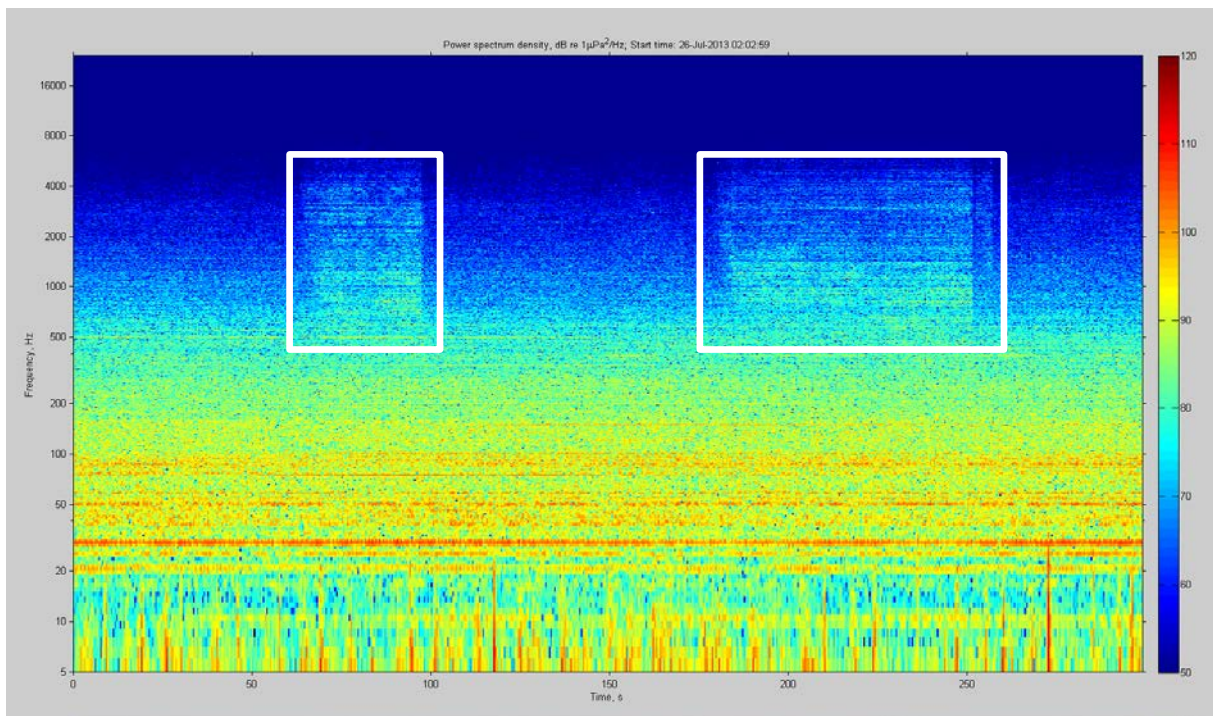


Figure 29: Frequency analysis of unidentified sounds (white boxes) recorded on 26 July 2013. The power spectrum density (colour-coded, see legend on the right) is integrated over 1 s, displayed in dB re $1\mu\text{Pa}^2/\text{Hz}$ and plotted as a function of frequency (in logarithmic units) over time.

Quantitative analysis of noise levels

Spatial differences

The quantitative analysis of ambient noise was conducted using a custom Matlab script. A representative example of the results is given below for the recordings from station GEMINI 1 and 8 made in summer 2013. Figures 30 and 31 show the percentile spectral levels of ambient noise for the first recording period at both stations. Generally, the spectral levels decreased almost linearly with increasing frequency from 10 Hz to 24 kHz, which is a common characteristic of ambient noise spectral data.

In comparison the spectral analysis from station GEMINI 1 and 8 reveals no drastic differences in the sound scape at both sites. Station 1, situated further to the West, shows higher levels (5-10 dB) below 100 Hz, a frequency band normally dominated by flow noise from e.g. tidal currents. Also at frequencies between 200 and 800 Hz levels are elevated by 5-10 dB in the 5th -50th percentiles, indicating a higher contribution from nearby and distant shipping activity.

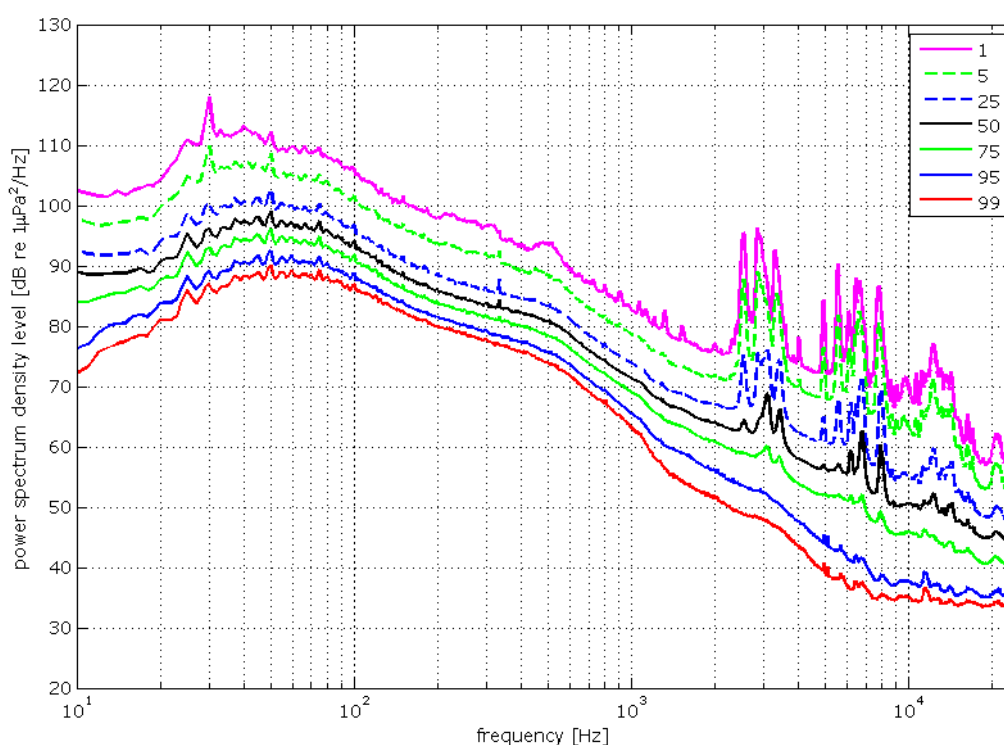


Figure 30: Percentile power spectral density levels (dB re 1 $\mu\text{Pa}^2/\text{Hz}$) for the entire recording period recorded at position 1/ AMAR 128. Spectral level percentiles: Histograms of each frequency bin (1 Hz) for all 1 min data from each recorder were computed. The 1st, 5th, 25th, 50th, 75th, 95th and 99th percentiles were plotted. The 99th percentile curve describes the frequency dependent levels exceeded by 99% of the 1 min averages. Equivalently, 99% of the 1 min spectral levels are below the 1st percentile curve. The 50% percentile is the median.

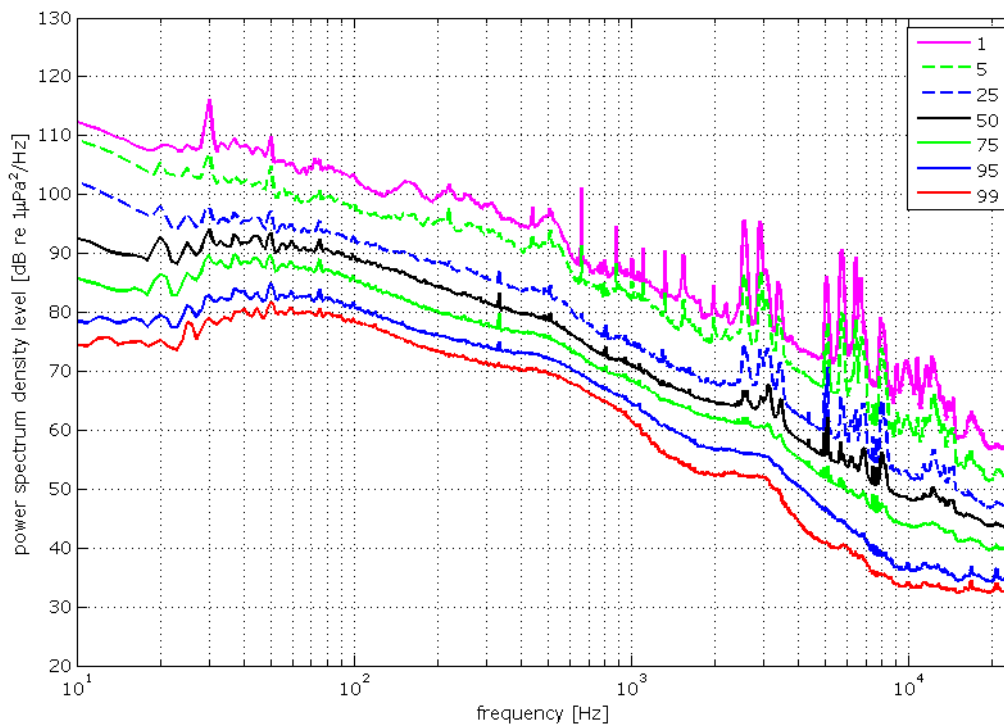


Figure 31: Percentile power spectral density levels (dB re 1 $\mu\text{Pa}^2/\text{Hz}$) for the entire recording period recorded at position 8/ AMAR 142 (x-axis: power spectrum density [dB re 1 $\mu\text{Pa}^2/\text{Hz}$], y-axis: frequency [Hz]). Spectral level percentiles: Histograms of each frequency bin (1 Hz) for all 1 min data from each recorder were computed. The 1st, 5th, 25th, 50th, 75th, 95th and 99th percentiles were plotted. The 99th percentile curve describes the frequency dependent levels exceeded by 99% of the 1 min averages. Equivalently, 99% of the 1 min spectral levels are below the 1st percentile curve. The 50% percentile is the median.

The 50th percentile can be compared to the Wenz ambient noise curves shown in Figure 3. The Wenz curves show ranges of variability of ambient spectral levels as a function of frequency based on measurements off the Pacific Coast of the United States. The analysis of ambient noise shows that the normal background noise level at both positions is higher than in offshore areas in undisturbed situations (Figure 3 in comparison to Figures 30 and 31).

While shipping activity with its almost continuous noise emission into the marine environment appears to be the single anthropogenic sound source contributing most to the local sound scape at both stations, pile driving noise also contributed significantly. For example, pile driving was present during at least 62 of the hours over the 18 day period between 18-07-2013 and 07-09-2013. With an average duration per impulse of 0.5 ms and a repetition interval of approximately 2 s, pile driving contributes to the soundscape only over a total of 15.5 h over these 18 days. However, behavioural effects on marine mammals do not depend on the duration of the individual signal, but the activity as such, i.e. the behavioural relevance of pile driving lasts longer (Daehne et al. 2013, Brandt et al. 2011). Consequently, the onset and ending of the activity needs to be taken into account in the analysis of the biological data (harbour porpoise and seal, behaviour and presence).

The quantitative analysis of the soundscape at GEMINI 8 for a pile driving period at a windpark at several (tens) kilometres distance as compared to a period without this activity clearly shows the increase in the frequency band between 400 Hz and 1 kHz in the 5th -50th percentiles by up to 20 dB (Figure 32).

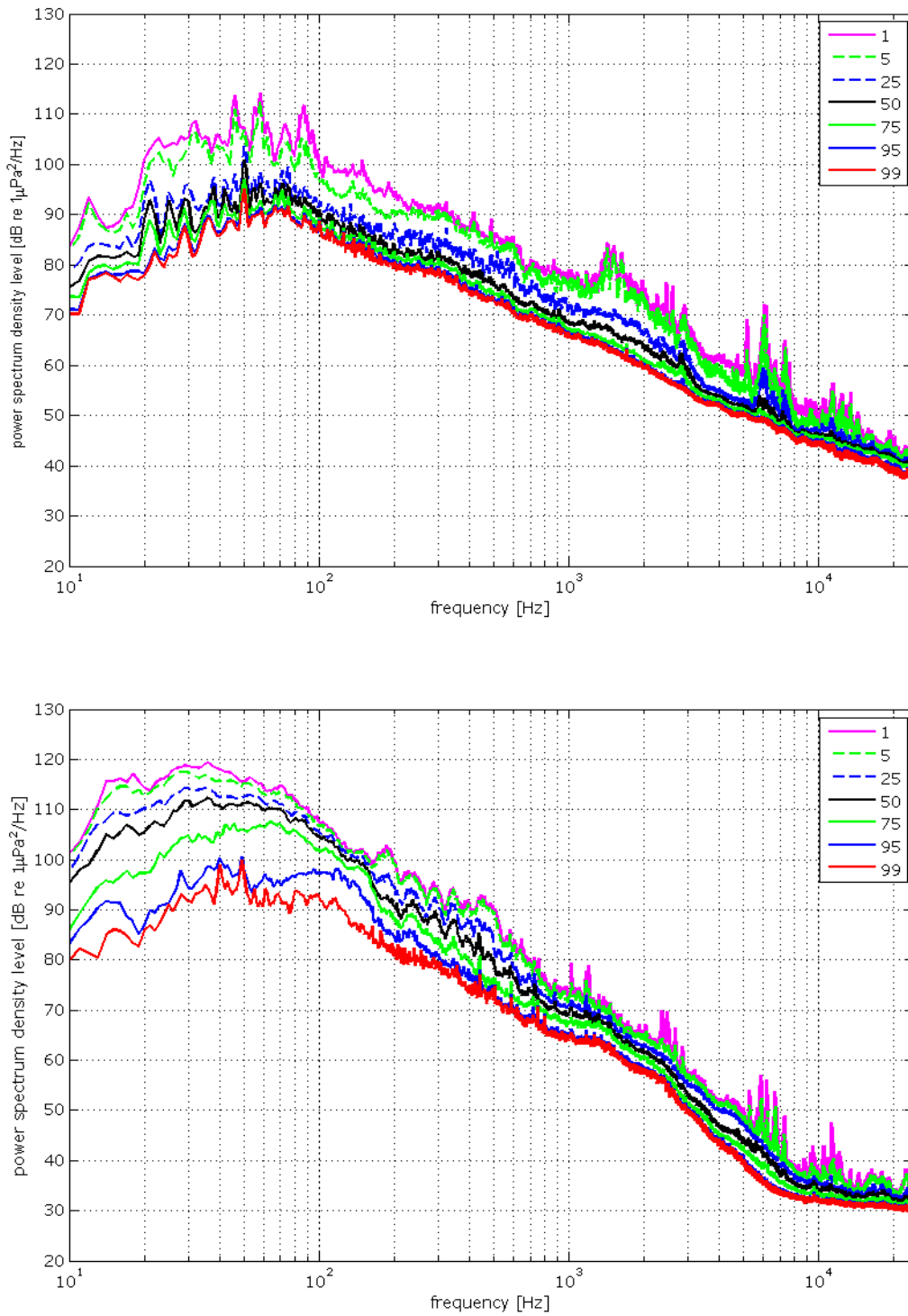


Figure 32: Comparison of percentile power spectral density levels (dB re 1 $\mu\text{Pa}^2/\text{Hz}$) for an 4.5 hour recording period without (upper graph) and with pile driving (lower graph) recorded at position 8 (AMAR 276) (x-axis: power spectrum density [dB re 1 $\mu\text{Pa}^2/\text{Hz}$], y-axis: frequency [Hz]). Spectral level percentiles: Histograms of each frequency bin (1 Hz) for all 1 min data from each recorder were computed. The 1st, 5th, 25th, 50th, 75th, 95th and 99th percentiles were plotted. The 99th percentile curve describes the frequency dependent levels exceeded by 99% of the 1 min averages. Equivalently, 99% of the 1 min spectral levels are below the 1st percentile curve. The 50% percentile is the median.

Seasonal differences

The quantitative analysis of the sound recordings shows insignificant differences between the months of the study period (Figure 33, 34). The levels vary 5-10 dB in general with only the tonal signature of shipping sound contributing to the soundscape by 15 dB more in September than in July 2013 and low frequency sound generated by tidal currents, especially in June 2014 at position GEMINI 8.

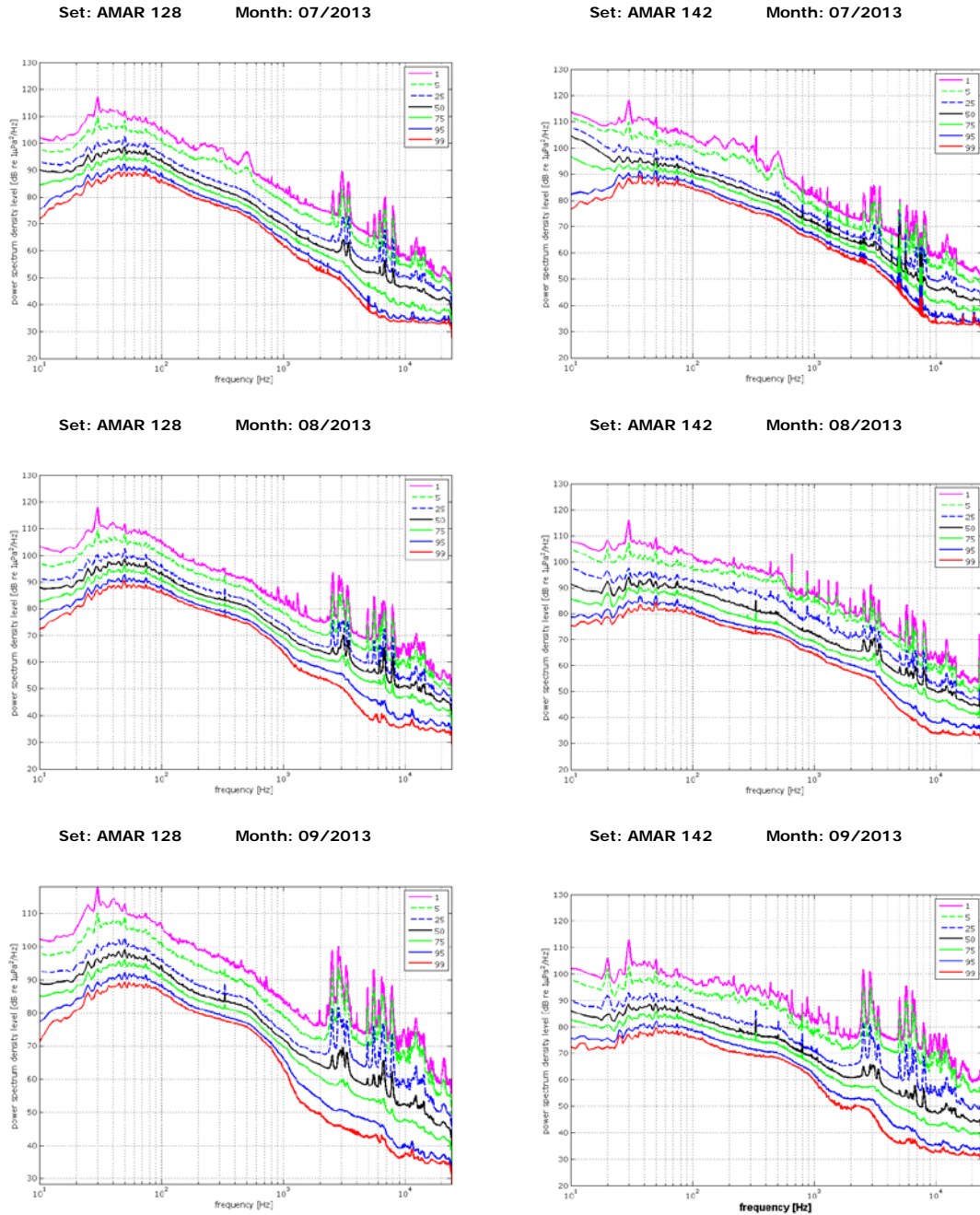


Figure 33: Comparison of percentiles per month (July-September 2013) for position GEMINI 1/ AMAR 128 (left) and position GEMINI 8/ AMAR 142 (right) (x-axis: power spectrum density [dB re 1 $\mu\text{Pa}^2/\text{Hz}$], y-axis: frequency [Hz]). Spectral level percentiles: Histograms of each frequency bin (1 Hz) for all 1 min data from each recorder were computed. The 1st, 5th, 25th, 50th, 75th, 95th and 99th percentiles were plotted. The 99th percentile curve describes the frequency dependent levels exceeded by 99% of the 1 min averages. Equivalently, 99% of the 1 min spectral levels are below the 1st percentile curve. The 50% percentile is the median.

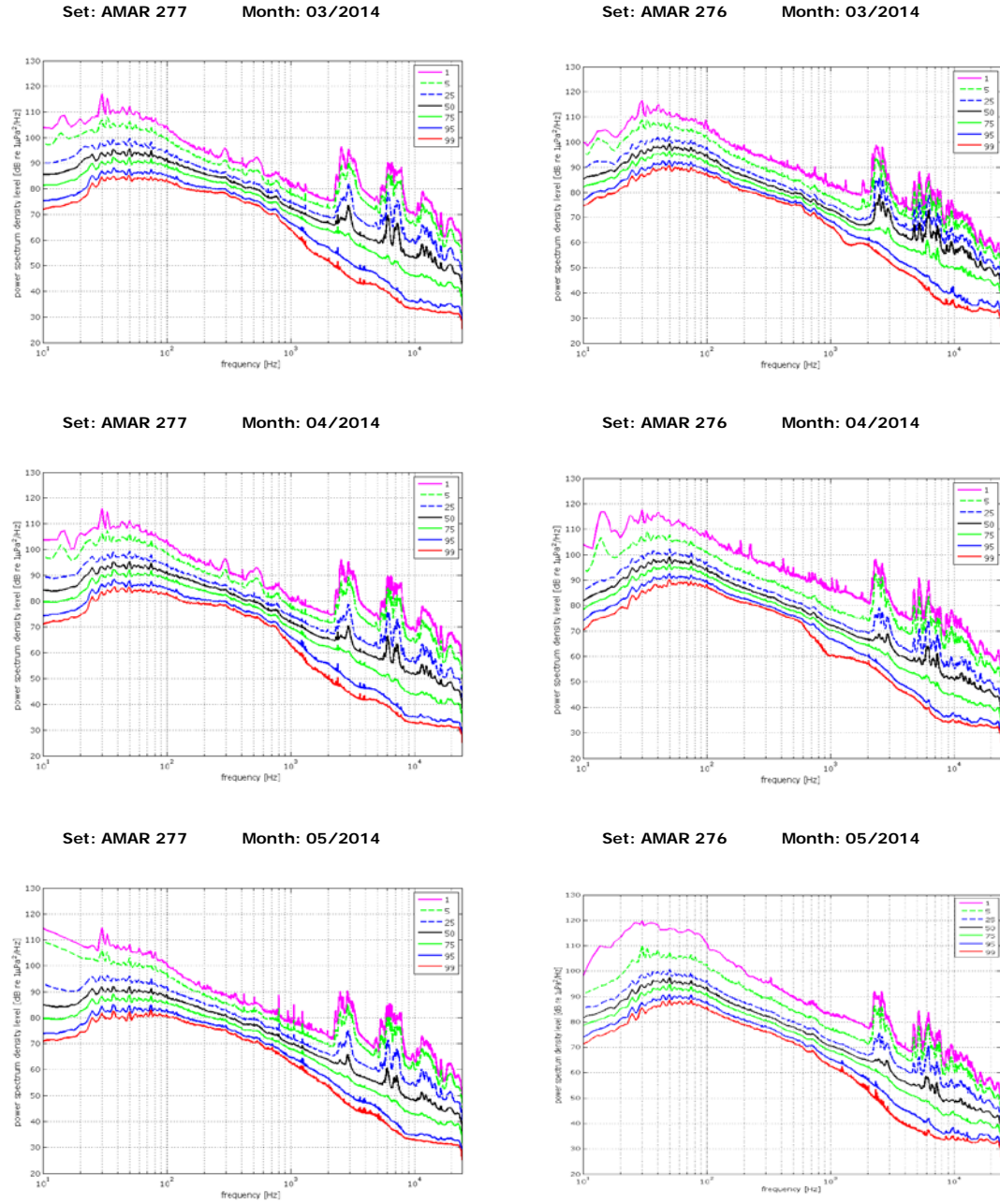
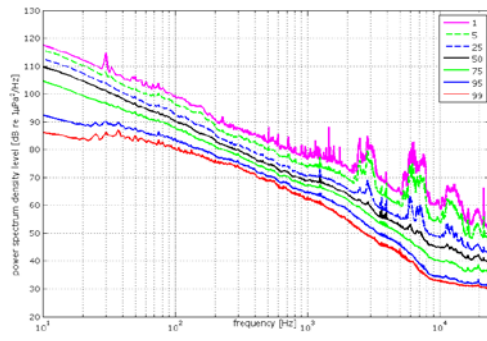


Figure 34: Comparison of percentiles per month (March-June, contd. on following page) for position GEMINI 1/ AMAR 277 (left) and position GEMINI 8/ AMAR 276 (right) (x-axis: power spectrum density [dB re $1 \mu\text{Pa}^2/\text{Hz}$], y-axis: frequency [Hz]). Spectral level percentiles: Histograms of each frequency bin (1 Hz) for all 1 min data from each recorder were computed. The 1st, 5th, 25th, 50th, 75th, 95th and 99th percentiles were plotted. The 99th percentile curve describes the frequency dependent levels exceeded by 99% of the 1 min averages. Equivalently, 99% of the 1 min spectral levels are below the 1st percentile curve. The 50% percentile is the median.

Set: AMAR 277 Month: 06/2014



Set: AMAR 276 Month: 06/2014

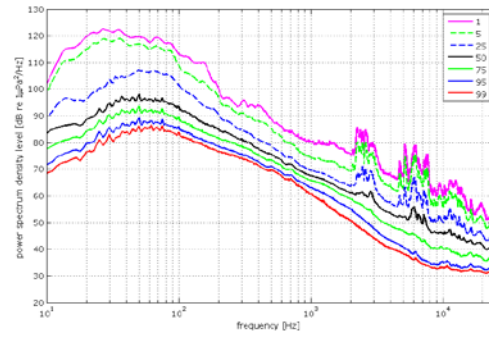


Figure 34. Continued.

Discussion

During the construction and operation of renewable energy devices many activities can be identified which may, due to their emissions, have an effect on marine animals. High level emissions such as those produced during pile driving in the construction phase may cause hearing damage at close range, whereas noise emissions during the operational phase may cause masking of biologically significant signals. These can cause stress as well as disturbance to marine animals eliciting behavioural responses such as avoidance (Brandt et al. 2011, Daehne et al. 2013) which leads to the potential for habitat exclusion. Long-term effects of chronic exposure of marine animals to anthropogenic noise are of considerable current interest, although research in this field is limited (e.g. Popper and Hastings 2009, Slabbekoorn et al. 2010, Normandeau Associates, Inc. 2012).

The environmental impact associated with the construction and operation of offshore wind facilities has led to a substantial amount of measurement work, particularly related to water-borne radiated noise. This has included measurements of the acoustic pressure in the water during offshore wind projects in both the construction phase (predominantly impact pile driving) (e.g. Robinson et al., 2009; Bailey et al., 2010; Robinson et al., 2011; Ainslie et al. 2012) and operational phases (Madsen et al. 2006; Tougaard et al. 2009; Nedwell et al. 2011; Sigray et al. 2011). These studies allow a sufficiently robust characterisation of offshore pile driving sounds in general, but are limited in time and are site specific as far as the soundscape is concerned.

The sound measurements conducted by IMARES, using state-of-the-art noise loggers, provide unique data sets of the underwater soundscape at the GEMINI site and a reference for the area as they were conducted over long periods and can be directly linked with studies on marine mammal behaviour in the construction study area. Such data are essential for the assessment of potential effects of the construction and operation of the GEMINI windpark on marine mammals.

The data recorded during the T0 phase comply with the requirements given by the EU Marine Strategy Framework Directive adopted to achieve Good Environmental Status (GES) by 2020 as well as national standards (e.g. de Jong et al. 2011, TSG Noise 2013). The increasing concern about offshore developments effecting marine life has led to legislation at both the European and national level (e.g. EU Habitats' Directive 92/43/EC, EIA Directive 2011/92/EU and the SEA Directive 2001/42/EC). Environmental monitoring is routinely required over the entire sequence of baseline, construction and operational phases, but sufficient understanding is not yet available with regard to the impact on marine fauna.

In order to understand the level and nature of newly introduced sound into the marine environment by the construction of the GEMINI wind turbines it is essential to first have a solid baseline. The recorded noise provides this back-ground to which will be added the Gemini pile driving and other construction-related sounds in 2015. This can be expected to cause behavioural reactions in marine mammals as well as fishes and other taxa.

Conclusion

The sounds recorded and identified comprise natural sounds produced by tidal currents and rain as well as several anthropogenic sounds. The most common sound source is shipping, leading to varying sound levels and spectra at the two noise logger stations, depending on the distance and type of shipping. While shipping sound is almost constantly present, underwater explosions and pile driving impulses are the most relevant types of anthropogenic sounds in terms of their source levels and both have extremely long propagation ranges. While explosions were only identified a few times, pile driving sounds were present over several weeks during the study period. In the context of this study, the identification and quantification of these two transient types of sounds are of special relevance as they have the largest potential for disturbing marine mammals (Richardson et al. 1995). The current findings provide already a key parameter for the analysis of information on the presence and behaviour of marine mammals during the T0 phase of the GEMINI windpark. Equally important, these data provide an excellent back-ground for assessing the potential effects of pile driving conducted during the construction phase in 2015. It is paramount to conduct similar underwater noise recordings during the construction period to enable interpretation of potential impacts. Without knowledge about the presence of a potentially disturbing

activity or imprecise temporal information the cause-effect, analysis can lead to false positive correlations and could under or over-estimate the effect of wind turbine related activities.

References

- Ainslie, M.A., de Jong, C.A.F., Dol, H.S., Blacqui re, G. and Marasini, C. (2009) Assessment of natural and anthropogenic sound sources and acoustic propagation in the North Sea. TNO report TNO-DV 2009 C085.
- Bailey, H., Senior, B., Simmons, D., Rusin, J., Picken, G. and Thompson, P. M. (2010) Assessing underwater noise levels during pile-driving at an offshore wind farm and its potential effects on marine mammals, *Marine Pollution Bulletin* 60: 888-897.
- Brandt, M., Diederichs, A., Betke, K., and Nehls, G. (2011). Responses of harbour porpoises to pile-driving at the Horns Rev II offshore wind farm in the Danish North Sea. *Marine Ecology Progress Series* 421: 205–16.
- Carey, W. M. (2009). Lloyd's Mirror—Image Interference Effects. *Acoustics Today* 5(2): 14-20. doi:10.1121/1.3182842)
- D hne, M., Gilles, A., Lucke, K., Peschko, V., Adler, S., Kr gel, K., Sundermeyer, J., and Siebert, U. (2013). Effects of pile-driving on harbor porpoise (*Phocoena phocoena*) at the first offshore wind farm in Germany. *Environmental Research Letters* 8: 1-17, doi: 10.1088/1748-9326/8/2/025002.
- De Jong, C.A.F., Ainslie, M.A., and Blacqui re, G. (2011). Standard for measurement and monitoring of underwater noise, Part II: procedures for measuring underwater noise in connection with offshore wind farm licensing, Report no. TNO-DV 2011 C251.
- Madsen, P.T., Wahlberg, M., Tougaard, J, Lucke, K. and Tyack P. (2006) Wind turbine underwater noise and marine mammals: implications of current knowledge and data needs. *Marine Ecology Progress Series* 309: 279-295.
- Merchant, N.D., Blondel, P., Dakin, D.T., and Dorocicz, J. (2012). Avergaing underwater noise levels for environmental assessment of shipping. *JASA Express Letters* 132(4): 343-349.
- Nedwell, J.R., Brooker, A.G., Edwards, B. and Bird, H. (2011). Subsea operational noise assessment of the Gunfleet Sands offshore wind farm, Subacoustech Report No. E267R0103, June 2011.
- Normandeau Associates, Inc. (2012) Effects of Noise on Fish, Fisheries, and Invertebrates in the U.S. Atlantic and Arctic from Energy Industry Sound-Generating Activities. A Workshop Report for the U.S. Dept. of the Interior, Bureau of Ocean Energy Management. Contract # M11PC00031. 72 pp. plus Appendices.
- Nystuen, J. A. (1986). Rainfall measurements using underwater ambient noise. *Journal of the Acoustical Society of America* 79(4): 972-982.
- Ocean Studies Board (2003). Ocean noise and marine mammals. National Academy Press, Washington D.C., 220 pp.
- Popper, A.N., and Hastings, M.C. (2009). The effects on fish of human-generated (anthropogenic) sound. *Integrative Zoology* 4: 43-52.
- Richardson, W.J., Greene, C.R.J., Malma, C.I., and Thomson, D.H. (1995). *Marine Mammals and Noise*. Academic Press, San Diego, CA.
- Robinson, S.P., Lepper, P.A., Ablitt, J., Hayman, G., Beamiss, G.A., Theobald, P.D. and Dible, S. (2009). A methodology for the measurement of radiated noise from marine piling, *Proceedings of the 3rd International Conference & Exhibition on "Underwater Acoustic Measurements: Technologies & Results"*, Napfion, Greece, June 2009.
- Robinson, S.P., Theobald, P.D. and Lepper, P.A. (2011). The noise radiate by marine piling for the construction of offshore wind farms. *Proceedings of the 4th International Conference & Exhibition on "Underwater Acoustic Measurements: Technologies & Results"*, Kos, Greece, 2011.
- Sigray, P. and Andersson, M.H. (2011). Particle motion measured at an operational wind turbine in relation to hearing sensitivity in fish. *Journal of the Acoustical Society of America* 130: 200-207.
- Slabbekoorn, H., Bouton, N., Opzeeland, I. van, Coers, A., Cate, C. ten and Popper, A.N. (2010) A noisy spring: the impact of globally rising underwater sound levels on fish. *Trends in Ecology and Evolution* 25: 419-427.

Tougaard, J., Henriksen, O.D. and Miller, L.A. (2009). Underwater noise from three types of offshore wind turbines: Estimation of impact zones for harbor porpoises and harbor seals. *Journal of the Acoustical Society of America* 125: 3766-3773.

Monitoring Guidance for Underwater Noise in European Seas - 2nd Report of the Technical Subgroup on Underwater noise (TSG Noise). Part I – Executive Summary. Interim Guidance Report. May, 2013.

Wenz, G.M. (1962). Acoustic ambient noise in the ocean: Spectra and sources. *Journal of the Acoustical Society of America* 34: 1936-1956.

Appendix A

Glossary

Units

Bft	Beaufort
dB	Decibel
Hz	Hertz
kHz	Kilohertz
Pa	Pascal
µPa	Micro-Pascal

Acoustic Terms

Acoustic Pressure	The force per unit area exerted by a sound wave above and below the ambient or static equilibrium pressure is called the acoustic pressure or sound pressure. The units of pressure are pounds per square inch (psi) or, in the SI system of units, Pascals [Pa].
Ambient noise	The background noise in an area or environment being a composite of noise from many sources, near and far.
Amplitude	The maximum positive and negative deviation of a wave, e.g. a sound wave.
Anthropogenic Effects	Processes, objects, energy, or materials that are derived from human activities, as opposed to those occurring naturally.
Anthropogenic noise	Collective for all human produced sources of unwanted sound.
Beaufort	Scale for classification of wind speed – the Beaufort scale.
dB re 1 µPa	Decibel referenced to 1 micro-Pascal
dB re 1 µPa ² .s	Decibel referenced to 1 micro-Pascal squared, times time in seconds
Decibel	[dB]; a logarithmic scale for describing differences in e.g. sound pressure relative to a reference pressure. In underwater acoustics the standard reference is one-millionth of a Pascal, called a micro-Pascal (1 µPa). The dB symbol is followed by a second symbol identifying the specific reference value (i.e., re 1 µPa). Decibel is a dimensionless ratio term that can be applied to any two values. Decibels are expressed as 10 times the logarithm of the ratio of a value (V) to its reference value (Vref), or: N decibels (dB) = 10*log (V/Vref). Decibels should always be accompanied by their reference value that defines the ratio being expressed unless clearly specified in the beginning. (In this report all references to dB that are not accompanied by a specific reference value are dB of Sound Pressure Level , referenced to 1 micro-Pascal of pressure).
Emission vs. Immission	With regards to exposure to sound, 'emission' refers to sound from the source and 'immission' refers to sound received by a person or animal.
Fast Fourier Transform	FFT; transforms digitised waveforms to the frequency domain.
FFT	See 'Fast Fourier Transform'
Frequency bandwidth	The range of frequencies over which a sound is produced or received.
Frequency spectrum	See Spectrum.

Hertz	Hz; the unit of frequency where 1 Hertz = 1 cycle per second. The range of human hearing stretches between 20-20.000 Hz.
HF	High-frequency
Immission	See 'Emission vs. Immission'.
Impulse	See Impulse sound.
Impulsive sound	Transient sound produced by a rapid release of energy, usually electrical, mechanical or chemical such as circuit breakers, airguns or explosives. There are no clear boundaries between impulse sounds and tonal ('continuous') sounds, but generally speaking impulse sounds are 1) of short duration (less than 1 second, and usually much shorter), and 2) have an irregular waveform, rather than the smooth sinusoidal waveform generated by most sonars or speech, for example.
Infrasound	Sound at frequencies below the hearing range of humans. These sounds have frequencies below about 20 Hz.
Kilohertz	1000 Hz (see Hertz)
LF	low-frequency
Lloyd's mirror interference	An acoustic source just below the water surface generates constructive and destructive interference between the direct path and reflected paths (Wikipedia). Interference due to Lloyd's mirror results in low frequency sounds not being discernible near the surface. This is because at the surface, sound reflections are nearly 180 degrees out of phase with the incident waves.
MF	mid-frequency
OWT	Offshore wind turbine
Peak pressure	The highest pressure above or below ambient that is associated with a sound wave.
Pinger	Autonomous battery powered electronic device producing sound patterns in random or constant time intervals. Developed to deter cetaceans from gillnets. Also used as reference source for hydrophone arrays or as acoustic measurements.
Propagation loss	Transmission losses of sound over distance through a medium (air, seawater). The propagation losses of sound are frequency-dependend and also depend on complex number of factors (bottom structure, sediment, etc.) and are mostly irregular in coastal waters. In the far-field of a sound source the rate of decrease is proportional to the distance $1/r$. In an unbounded, homogenous medium, propagation loss will be on the order of 6 dB for every doubling of the distance.
Pulse	See Impulse sound.
Receive Level	RL; the Receive Level is the Sound Pressure Level of a sound measured at a receiver (e.g. an animal or a hydrophone).
Rise time	The interval of time required for a signal to go from zero, or its lowest value, to its maximum value. Frequency spreading and environmental scattering would tend to 'smear' the rise time as the sound propagated away from the source.
Root-mean-square amplitudes	rms; these amplitudes include an averaging of the pressure wave signal over a certain time window. For sinusoidal signals, the rms pressure is usually about 9 dB lower than the peak-to-peak pressure.
Shock wave	A propagating sound wave where the amplitude of the field is so large that the linear approximation to the governing physics equations is no longer valid and where discontinuities in acoustic quantities such as pressure and particle velocity can occur.
Sonar	Sonar (Sound Navigating And Ranging) may be active or passive. Active sonar projects a sound and then listens for echoes of that sound returning from underwater objects. Passive sonar does not project a sound, but instead only listens for sounds produced by underwater objects.
Sound attenuation	Reduction of the level of sound pressure. Sound attenuation occurs naturally as a wave travels in a fluid or solid through dissipative processes (e.g., friction) that

	convert mechanical energy into thermal energy and chemical energy.
Sound exposure level	SEL; the constant sound level acting for one second, which has the same amount of acoustic energy, as indicated by the square of the sound pressure, as the original sound. It is the time-integrated, sound-pressure-squared level. SEL is typically used to compare transient sound events having different time durations, pressure levels, and temporal characteristics. It is given dB re 1 $\mu\text{Pa}^2\cdot\text{s}$.
Sound Pressure Level (SPL)	SPL; the Sound Pressure Level of a sound source measured at a certain distance from a sound source and commonly referred to a reference pressure level of 1 μPa and expressed in dB re 1 μPa .
Source level	SL; the Source level is the Sound Pressure Level of a sound source measured on the acoustic axis at a distance of 1 m from the source. In underwater acoustics this level is commonly referred to a reference pressure of 1 μPa . The definition is then 10 log intensity, divided by the reference intensity and expressed in dB (decibel) re (relative to) 1 μPa at 1 m.
Spectrogram	A graph, which displays acoustic energy as a function of frequency allowing frequency patterns to be visualised, and reverberations to be depicted.
Spectrum	A graphical display of the contribution of each frequency component contained in a sound.
SPL	Sound pressure level
Threshold	The threshold generally represents the lowest signal level an animal will detect in some statistically predetermined percent of presentations of a signal.
Transducer	A device (hydrophone e.g.) to convert underwater sound into electrical voltage.
Ultrasound	Sound at frequencies above the hearing range of humans. These sounds have frequencies above about 20 Hz.
Propagation (sound propagation)	Several factors must be considered when reviewing the acoustic propagation reported here. First, there is a difference between Source Level (SL), measured at one meter from the acoustic centre the source, and Receive Level (RL), the amount of sound an animal would receive at some distance from the source. Due to spherical spreading of sound, absorption, reflection, scattering, and other phenomena, Receive Levels drop markedly as one moves away from the source. For example, a Source Level of 235 dB one meter from the source dissipates to a Receive Level of 180 dB at a distance of 200 m to 1000 m from the source, depending on conditions.